Atmos. Chem. Phys., 17, 551–574, 2017
www.atmos-chem-phys.net/17/551/2017/
doi:10.5194/acp-17-551-2017

Atmospheric Chemistry and Physics
Open Access
EGU

Detecting volcanic sulfur dioxide plumes in the Northern Hemisphere using the Brewer spectrophotometers, other networks, and satellite observations

Christos S. Zerefos[1,2,3,4], Kostas Eleftheratos[2,5], John Kapsomenakis[1], Stavros Solomos[6], Antje Inness[7], Dimitris Balis[8], Alberto Redondas[9], Henk Eskes[10], Marc Allaart[10], Vassilis Amiridis[6], Arne Dahlback[11], Veerle De Bock[12], Henri Diémoz[13], Ronny Engelmann[14], Paul Eriksen[15], Vitali Fioletov[16], Julian Gröbner[17], Anu Heikkilä[18], Irina Petropavlovskikh[19], Janusz Jarosławski[20], Weine Josefsson[21], Tomi Karppinen[22], Ulf Köhler[23], Charoula Meleti[8], Christos Repapis[4], John Rimmer[24], Vladimir Savinykh[25], Vadim Shirotov[26], Anna Maria Siani[27], Andrew R. D. Smedley[24], Martin Stanek[28], and René Stübi[29]

[1]Research Centre for Atmospheric Physics and Climatology, Academy of Athens, Athens, Greece
[2]Biomedical Research Foundation, Academy of Athens, Athens, Greece
[3]Navarino Environmental Observatory (N.E.O.), Messinia, Greece
[4]Mariolopoulos-Kanaginis Foundation for the Environmental Sciences, Athens, Greece
[5]Faculty of Geology and Geoenvironment, National and Kapodistrian University of Athens, Athens, Greece
[6]Institute for Astronomy, Astrophysics, Space Applications and Remote Sensing (IAASARS), National Observatory of Athens, Athens, Greece
[7]European Centre for Medium-Range Weather Forecasts (ECMWF), Reading, UK
[8]Department of Physics, Aristotle University of Thessaloniki, Thessaloniki, Greece
[9]Izaña Atmospheric Research Center, AEMET, Tenerife, Canary Islands, Spain
[10]Royal Netherlands Meteorological Institute (KNMI), De Bilt, the Netherlands
[11]Department of Physics, University of Oslo, Oslo, Norway
[12]Royal Meteorological Institute of Belgium, Brussels, Belgium
[13]ARPA Valle d'Aosta, Saint-Christophe, Italy
[14]Leibniz Institute for Tropospheric Research, Leipzig, Germany
[15]Danish Meteorological Institute, Copenhagen, Denmark
[16]Environment and Climate Change Canada, Toronto, Canada
[17]PMOD/WRC, Davos Dorf, Switzerland
[18]Climate Change Unit, Finnish Meteorological Institute, Helsinki, Finland
[19]Cooperative Institute for Research in Environmental Sciences, University of Colorado, Boulder, CO, USA
[20]Institute of Geophysics, Polish Academy of Sciences, Warsaw, Poland
[21]Swedish Meteorological and Hydrological Institute, Norrköping, Sweden
[22]Arctic Research Centre, Finnish Meteorological Institute, Sodankylä, Finland
[23]DWD, Meteorological Observatory Hohenpeißenberg, Hohenpeißenberg, Germany
[24]Centre for Atmospheric Science, School of Earth, Atmospheric and Environmental Sciences, University of Manchester, Manchester M13 9PL, UK
[25]A.M. Obukhov Institute of Atmospheric Physics, Kislovodsk, Russia
[26]Institute of Experimental Meteorology, Obninsk, Russia
[27]Department of Physics, Sapienza, University of Rome, Rome, Italy
[28]Solar and Ozone Observatory, Czech Hydrometeorological Institute, Hradec Králové, Czech Republic
[29]Federal Office of Meteorology and Climatology, MeteoSwiss, Payerne, Switzerland

Correspondence to: Christos S. Zerefos (zerefos@geol.uoa.gr)

Published by Copernicus Publications on behalf of the European Geosciences Union.

Received: 11 June 2016 – Published in Atmos. Chem. Phys. Discuss.: 4 July 2016
Revised: 1 December 2016 – Accepted: 12 December 2016 – Published: 11 January 2017

Abstract. This study examines the adequacy of the existing Brewer network to supplement other networks from the ground and space to detect SO_2 plumes of volcanic origin. It was found that large volcanic eruptions of the last decade in the Northern Hemisphere have a positive columnar SO_2 signal seen by the Brewer instruments located under the plume. It is shown that a few days after the eruption the Brewer instrument is capable of detecting significant columnar SO_2 increases, exceeding on average 2 DU relative to an unperturbed pre-volcanic 10-day baseline, with a mean close to 0 and $\sigma = 0.46$, as calculated from the 32 Brewer stations under study. Intercomparisons with independent measurements from the ground and space as well as theoretical calculations corroborate the capability of the Brewer network to detect volcanic plumes. For instance, the comparison with OMI (Ozone Monitoring Instrument) and GOME-2 (Global Ozone Monitoring Experiment-2) SO_2 space-borne retrievals shows statistically significant agreement between the Brewer network data and the collocated satellite overpasses in the case of the Kasatochi eruption. Unfortunately, due to sparsity of satellite data, the significant positive departures seen in the Brewer and other ground networks following the Eyjafjallajökull, Bárðarbunga and Nabro eruptions could not be statistically confirmed by the data from satellite overpasses. A model exercise from the MACC (Monitoring Atmospheric Composition and Climate) project shows that the large increases in SO_2 over Europe following the Bárðarbunga eruption in Iceland were not caused by local pollution sources or ship emissions but were clearly linked to the volcanic eruption. Sulfur dioxide positive departures in Europe following Bárðarbunga could be traced by other networks from the free troposphere down to the surface (AirBase (European air quality database) and EARLINET (European Aerosol Research Lidar Network)). We propose that by combining Brewer data with that from other networks and satellites, a useful tool aided by trajectory analyses and modelling could be created which can also be used to forecast high SO_2 values both at ground level and in air flight corridors following future eruptions.

1 Introduction

Volcanic eruptions are an important source of natural emissions of sulfur dioxide (SO_2) into the troposphere and the stratosphere. Ash particles and gases injected into the atmosphere by large volcanic eruptions can affect solar radiation and climate (e.g. Robock, 2000) and air quality (e.g. Schmidt et al., 2015) and may also impact local environments (e.g. Durant et al., 2010). Volcanic emissions (e.g. ash and SO_2) can reach different heights in the atmosphere and can be transported in different directions (e.g. Prata et al., 2010). Thomas and Prata (2011) have shown that the eruption can be divided into an initial ash-rich phase, a lower-intensity middle phase and a final phase where considerably greater quantities of both ash and SO_2 are released, which in the case of ash can result in air travel disruptions (e.g. Flentje et al., 2010). These effects make the ash and SO_2 in volcanic plumes important parameters to be studied, monitored and forecasted on small and larger spatial scales. Our study focuses on volcanic columnar SO_2 amounts because of the existence of the fairly continuous set of direct sun measurements with the Brewer network.

Measurements of SO_2 are important for tracking and assessing impacts of emissions from pollution sources and in quantifying natural SO_2 emissions by volcanoes. Pollution sources typically result in a few Dobson unit (DU, $1\,\mathrm{DU} = 2.69 \times 10^{26}\,\mathrm{molec\,km^{-2}}$) increases in column SO_2 amounts unless observations are made near a source. The Brewer network is useful for plume tracking because it can track SO_2 columnar amounts from a large number of stations and wide geographical extent. The primary application of the ground-based Brewer spectrophotometer is to measure total ozone column by using UV spectrophotometry. Direct sunlight intensities are measured at five wavelengths (between 306 and 320 nm; see also Sect. 2.1) to simultaneously calculate ozone and SO_2 column integrals (Kerr et al., 1980). These instruments have been used extensively to monitor stratospheric ozone (e.g. WMO Scientific Assessment of Ozone Depletion reports, 2011, 2014) and have a long history of studying atmospheric SO_2 columns (e.g. De Backer and De Muer, 1991; Bais et al., 1993; Fioletov et al., 1998; Zerefos et al., 2000, 2009; Ialongo et al., 2015). Ground-based measurements of atmospheric SO_2 using the Brewer instrument have played an important role in the development and validation of satellite-based SO_2 measurements (Schaefer et al., 1997; Spinei et al., 2010; Rix et al., 2012; Ialongo et al., 2015) used primarily for detecting and tracking volcanic emissions. Since the Brewer instruments are located at stationary ground-based monitoring sites, a volcanic plume of SO_2 must pass over the site if useful data are to be obtained. Validation of satellite measurements by the Brewer instrument also requires that a satellite overpass is available when the plume is over the ground-based site (Kerr, 2010).

There have been various initiatives during recent years that used satellite measurements of SO_2 to monitor volcanic eruptions in support of aviation safety, e.g. ESA's Support to Aviation Control Service (SACS) (Brenot et al., 2014). These initiatives together with modelling forecasting

Table 1. Volcanic eruptions in the past decade considered in this study.

Volcano	Latitude	Longitude	Elevation (a.s.l.)	Period of eruption	VEI*
Okmok, Alaska	53.43° N	168.13° W	1073 m	12 July–19 August 2008	4
Kasatochi, Alaska	52.17° N	175.51° W	300 m	7–8 August 2008	4
Sarychev, Russia	48.1° N	153.2° E	1496 m	12–17 June 2009	4
Eyjafjallajökull, Iceland	63.63° N	19.62° W	1666 m	14 April–23 May 2010	4
Grímsvötn, Iceland	64.42° N	17.33° W	1725 m	21–25 May 2011	4
Nabro, Africa	13.37° N	41.70° E	2218 m	12–13 June 2011	4
Tolbachik, Russia	55.83° N	160.33° E	3611 m	27 November 2012–22 August 2013	4
Bárðarbunga, Iceland	64.64° N	17.56° W	2005 m	31 August 2014–28 February 2015	0

* Taken from the Smithsonian Institution Global Volcanism Program.

tools provide valuable information to the established Volcanic Ash Advisory Centers (VAAC). Satellite SO_2 data have been available in the past from various satellite instruments (e.g. GOME, SCIAMACHY). Currently operational data are available from UV measurements (e.g. GOME-2 (Global Ozone Monitoring Experiment-2), OMI (Ozone Monitoring Instrument) and OMPS (Ozone Mapping Profiler Suite)) and from infrared measurements (e.g. IASI (Infrared Atmospheric Sounding Interferometer) and AIRS (Atmospheric Infrared Sounder)).

In the present work we investigate the efficiency of the existing Brewer network in the Northern Hemisphere to detect volcanic SO_2 plumes during the past decade. The main focus is to show the sensitivity of the Brewer network in detecting SO_2 plumes of volcanic origin in synergy with other ground-based observations, satellite data and dynamic transport calculations. The Brewer spectroradiometric measurements are compared to collocated satellite measurements from OMI and GOME-2 as described in the next paragraph. This paper did not include analyses of the SO_2 measurements from IASI and AIRS since both instruments are IR spectroradiometers. We compared Brewer measurements to the OMI and GOME-2 data that are derived using information from differential optical absorption in the UV spectrum, which also forms the basis of the Brewer measurement methodology. In the case of Brewer–IASI or Brewer–AIRS comparison we would also have to consider differences in the spectroscopy and the corresponding retrieval algorithm concepts, which would require further analysis which is beyond the scope of this paper.

Table 1 lists in chronological order all major volcanic eruptions in the Northern Hemisphere between 2005 and 2015 with a volcanic explosivity scale index (VEI) of at least 4 (Newhall and Self, 1982; Robock, 2000; Zerefos et al., 2014). The study also provides a separate analysis for the Bárðarbunga eruption, which although not rated 4 has been already studied with the Brewer instrument at Sodankylä by Ialongo et al. (2015).

As seen from Table 1, chronologically, the first case was the volcanic eruption at Mount Okmok, Alaska (53.43° N, 168.13° W; 1073 m above sea level (a.s.l.); 12 July 2008; Prata et al., 2010) followed by the Kasatochi eruption, Alaska (52.17° N, 175.51° W; 300 m a.s.l.; 7–8 August 2008; e.g. Kristiansen et al., 2010; Krotkov et al., 2010; Waythomas et al., 2010), which was detected over large areas of the Northern Hemisphere. Okmok and Kasatochi volcanoes in Alaska erupted for a short time span of less than a month, and therefore we decided to study the evolution of the Brewer SO_2 columnar measurements following the latter volcanic eruption (Kasatochi). The third eruption took place at Sarychev in Russia (48.1° N, 153.2° E; 1496 m a.s.l.; 12–17 June 2009; Haywood et al., 2010). The evolution of the SO_2 volcanic plume from Sarychev was mostly observed over the North Pacific, North America and North Atlantic (Haywood et al., 2010). There was only one North American Brewer station (Saturna Island) in the path of the plume from Sarychev eruption. The record shows SO_2 columns of 8.6 DU detected on 19 June 2009 and 3.7 DU on 20 June 2009. This volcanic eruption is not investigated any further in this paper. The next eruption on the list, Eyjafjallajökull in Iceland (63.63° N, 19.62° W; 1666 m a.s.l.; from 14 April to 23 May 2010), resulted in interruption of the air traffic over NW Europe (e.g. Flemming and Inness, 2013). The fifth eruption Grímsvötn 2011 (64.42° N, 17.33° W; 1725 m a.s.l.; 21 May 2011) was studied by Flemming and Inness (2013), and by Moxnes et al. (2014). This eruption provided an interesting example of a clear separation of the volcanic SO_2 plume (transported mostly northwestward), while the fine ash was transported mostly southeastward. Unfortunately the volcanic plume did not overpass any Brewer station, and therefore we do not include any results post Grímsvötn eruption. The sixth eruption recorded features the Nabro in Africa (13.37° N, 41.70° E; 2218 m a.s.l.), which occurred on 12–13 June 2011 (e.g. Bourassa et al., 2012; Sawamura et al., 2012; Clarisse et al., 2014). We present here a case study that described the detection of the Nabro volcanic SO_2 plume over ground-based stations. The plume was clearly detected by the Brewer instrument over Izaña (and poorly from space), then over Taiwan by both Brewer and satellite instruments, and finally at Mauna Loa, Hawaii (mostly by the Brewer instrument). The seventh eruption was Tolbachik, Russia

(55.83° N, 160.33° E; 3.611 m a.s.l.), on 27 November 2012 (e.g. Telling et al., 2015). As in the case of Grímsvötn, the plume has not passed over any Brewer station that was verified by trajectory analysis. The next eruption on the list is the volcanic eruption from Bárðarbunga, Iceland (64.64° N, 17.56° W; 2005 m a.s.l.) that was observed between 31 August 2014 and 28 February 2015 (e.g. Schmidt et al., 2015). This last eruption, although not yet rated on the VEI scale, has been extensively studied in view of the observed increased SO_2 concentrations that have been observed all the way through the troposphere and reaching down to the surface in Europe (Ialongo et al., 2015; Schmidt et al., 2015).

The capability of the Brewer network to measure columnar SO_2 amounts above the local air pollution levels is also presented and discussed. The qualitative evidence that the plume can be detected in many single cases by the Brewer network has been quantitatively tested by calculating correlation coefficients with collocated satellite data. Only in the case of the Kasatochi 2008 eruption was it possible to test the sensitivity of SO_2 abundance measured by the Brewer spectrophotometers and from space. Correlations between the Brewer and collocated satellite SO_2 data from the Aura OMI and GOME-2 are presented in Sect. 3 where the correlation coefficients were found to be statistically significant at a confidence level of 99 %. For the other eruptions, unfortunately due to the sparsity of satellite data, no firm conclusions can be drawn, as discussed in Sect. 3.

The paper is structured in the following order. Sect. 2 describes the data sources and the methods of analysis of the columnar SO_2 measurements by the Brewer spectrophotometers (hereinafter simply referred to as the "Brewers"). Section 3 presents the analysis of the Brewer measurements during four of the volcanic eruptions listed in Table 1, along with satellite data and dynamic volcanic plume transport simulations. The conclusions are provided in Sect. 4.

2 Data and methods

2.1 Ground-based data

Sulfur dioxide in the atmosphere can be measured from ground-based instruments and by instrumentation onboard the spacecraft and can be estimated with the help of models. The Brewer is an automated, diffraction-grating spectrophotometer that provides observations of the sun's intensity in the near-UV range. The spectrophotometer measures the intensity of radiation in the ultraviolet absorption spectrum of ozone at five wavelengths (306.3, 310.1, 313.5, 316.8 and 320.1 nm) with a resolution of 0.6 nm. These data are used to derive the total ozone column (Kerr et al., 1980). Because sulfur dioxide has strong and variable absorption in this spectral region, the Brewer spectrophotometer has additionally been proposed to derive SO_2 columns (Kerr et al., 1980). About 200 Brewer spectrophotometers around the world contribute high-precision ozone data to the global ozone monitoring network (Kumharn et al., 2012). The existing Brewer network also delivers frequent SO_2 columnar measurements as well, which can be used for analyses, but with caution. This is because the signal-to-noise ratio for the SO_2 absorption is usually quite low and therefore well-calibrated instruments are required to monitor nominal SO_2 columnar amounts (Koukouli et al., 2014). Details on the method with which SO_2 is measured by the Brewer spectrophotometer can be found in Kerr et al. (1980, 1985, 1988) and De Backer and De Muer (1991). According to Fioletov et al. (2016), the uncertainty of the Brewer direct sun (DS) SO_2 measurements is about 1 DU and is typically insufficient for air quality applications. A more accurate method (with an uncertainty as low as 0.13 DU) based on Brewer "group-scan" spectral direct sun radiation measurements at 45 wavelengths from 306 to 324 nm was developed (Kerr, 2002) but not implemented for routine operations due to its complexity (Fioletov et al., 2016). Although the Brewer instrument has difficulties in detecting low columnar SO_2 concentrations, in extreme cases, such as volcanic eruptions, the SO_2 levels typically rise well above the instrumental noise and can be identified with the Brewer instrument as shown in this paper and in Fioletov et al. (1998).

Before proceeding to the analysis of Brewer measurements, the methodology to derive columnar SO_2 is first presented. To determine ozone and SO_2 column amounts, the measured raw photon counts at the five operational channels in the Brewer instrument are converted to radiation intensity. The Beer–Lambert absorption law is applied at each wavelength λ, and the measured intensity of direct sunlight is given by the following formula:

$$\log I_\lambda = \log I_{0\lambda} - \beta_\lambda \mu_\mathrm{R} - \delta_\lambda \mu_\mathrm{p} - \alpha_\lambda \mathrm{O_3} \mu - \sigma_\lambda \mathrm{SO_2} \mu, \quad (1)$$

where I_λ is the measured radiation intensity at wavelength λ, $I_{0\lambda}$ is the measured extraterrestrial spectrally resolved intensity at λ, β_λ is the Rayleigh scattering coefficient at λ, δ_λ is the particulate scattering coefficient at λ, α_λ is the ozone absorption coefficient (square centimetres per molecule) at λ, O_3 is the total ozone column (molecules per square centimetre), σ_λ is the SO_2 absorption coefficient at λ, SO_2 is the column amount of sulfur dioxide, μ_R, μ_p and μ are the optical path lengths (air masses) corresponding to the effective heights of molecules, particles and ozone respectively.

According to the Brewer retrieval algorithm, the following ratios are formed:

$$F = F_0 - \Delta\beta \mu_\mathrm{R} - \Delta\alpha \mathrm{O_3} \mu \quad (2)$$

and

$$F' = F'_0 - \Delta\beta' \mu_\mathrm{R} - \Delta\alpha' \mathrm{O_3} \mu - \Delta\sigma' \mathrm{SO_2} \mu, \quad (3)$$

where F is the weighted ratio of direct sun measurements at four (or six for double Brewer) spectral channels,

$F = \log I_2 - 0.5 \log I_3 - 2.2 \log I_4 + 1.7 \log I_5$, and F_0, $\Delta\beta$, and $\Delta\alpha$ are the same linear combinations for $\log I_{0\lambda}$, β_λ, and α_λ. The F' is the SO_2 ratio and $F' = \log I_1 - 4.2 \log I_4 + 3.2 \log I_5$ and F'_0, $\Delta\beta'$, $\Delta\alpha'$ and $\Delta\sigma'$ the corresponding linear combinations for $\log I_{0\lambda}$, β_λ, α_λ and σ_λ. Both of these functions have weights which eliminate the effects of particulate scattering, while the function F is weighted to remove SO_2 absorption effects as well. The extraterrestrial constants F_0 and F'_0 are determined from a long series of intercomparison measurements as well as zero air mass (μ) extrapolations.

The total ozone column is determined by the formula

$$O_3 = \frac{F_0 - F - \Delta\beta\mu_R}{\Delta\alpha\mu} \quad (4)$$

and the SO_2 by the formula

$$SO_2 = \frac{1}{A}\left(\frac{F'_0 - F' - \Delta\beta'\mu_R}{\Delta\alpha'\mu} - O_3\right), \quad (5)$$

where A is the ratio of the SO_2 absorption coefficient to the O_3 absorption coefficient; $A = 2.44$.

From the above-described operational Brewer algorithm it is evident that the estimation of columnar SO_2 is the result of the difference between two columnar terms ($O_3 + SO_2$) and O_3. Both terms have uncertainties (weighting functions, calibrations, random errors, systematic errors). Systematic negative values could be the result of a systematic offset in the measurements that can be related to the calibration of the instrument (usually optimized only for the ozone measurements). Randomly varying positive and negative values around zero, suggest that the signal of SO_2 is small (and thus the difference of two terms should be close to 0), but since both terms have uncertainties, negative values are possible, indicating that the amount of SO_2 in the atmosphere is below the detection limit of the instrument and could be considered as noise. In this work we have repeated our analysis excluding the negative values, and the results remained the same; i.e. a positive increase after a major volcanic eruption was confirmed as described in the following sections. Finally, we need to point out that perturbations by ash present in the volcanic plumes have been shown not to affect the Brewer SO_2 measurements. This is based on the result of the Pappalardo et al. (2013) paper based on EARLINET (European Aerosol Research Lidar Network) observations following the Eyjafjallajökull eruption, in which they found that the Ångström exponent of the volcanic ash optical depth is close to 0. This indicates that the effect of ash in the UV and visible region on the aerosol extinction is almost independent of wavelength. The Brewer SO_2 measurements taken in a narrow wavelength band in the UV are therefore not expected to be influenced by the presence of volcanic ash considering the weights already applied in the operational Brewer algorithm.

In this study we analysed 23 stations located in Europe, 6 Brewer stations in Canada, 2 in the USA and 1 in Taiwan; their geographical positions are shown in Fig. 1. SO_2 measurements were averaged over a large number of instruments

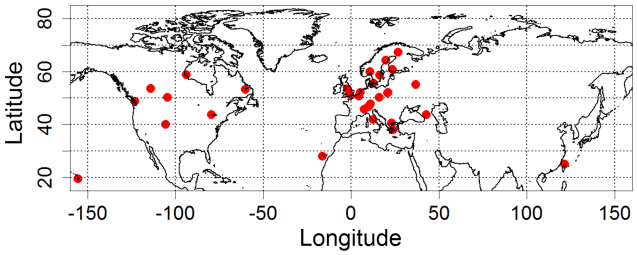

Figure 1. All stations with accessible SO_2 column data from Brewers analysed in this study as listed in Table 2.

and datasets during periods following volcanic eruptions. Random errors in the measurements of individual Brewer stations are reduced significantly by the averaging processes to calculate regional means.

Daily SO_2 columns at Churchill, Goose, Edmonton, Regina, Saturna Island and Toronto in Canada, T'aipei in Taiwan, and Boulder and Mauna Loa in the US were obtained from the World Ozone and Ultraviolet Radiation Data Centre (WOUDC; http://www.woudc.org/) and the NOAA-EPA Brewer Spectrophotometer UV and Ozone Network (NEUBrew; http://www.esrl.noaa.gov/gmd/grad/neubrew/). The data have been checked for quality assurance/quality control by the individual data providers. It is important to note the participation of most of the European Brewer data providers in a recent EU COST Action (EUBREWNET, http://www.eubrewnet.org/cost1207/) programme. Its focus is to establish a coherent network of European Brewer Spectrophotometer monitoring stations in order to harmonize operations and develop approaches, practices and protocols to achieve consistency in quality control, quality assurance and coordinated operations.

In our analysis only DS measurements satisfying the following criteria have been used: a Brewer DS measurement was included if and only if for every measurement cycle of five sets of measurements (from which also total columnar ozone is derived) the standard deviation of O_3 and SO_2 was less than 2.5 DU, the total columnar ozone was between 250 and 450 DU, and the solar zenith angle was less than 73.5°. To exclude erratic data of SO_2 from our analysis, values exceeding $\pm 6\sigma$ of the mean of all SO_2 individual Brewer measurements were considered erroneous and were not included in the calculations. Therefore, the range of analysed values was limited to a maximum of ± 35 DU for an individual measurement (i.e. 6σ, with σ being equal to 5.8 as estimated from all available sub-daily SO_2 values). Then we calculated daily SO_2 columns at each station only if at least three individual measurements passed these criteria for each day. Brewers are useful because they provide more than one observation per day. For plumes which change rapidly, more than one observation per day would be useful, especially to complement satellites which typically have just one local overpass.

Table 2. Stations with accessible SO_2 column data from Brewers analysed in this study. Stations are sorted from high to lower northern latitudes.

	Station	Latitude	Longitude	Elevation (m a.s.l.)	Instruments	Data source
1	Sodankylä	67.36	26.63	180	Brewer MKII 037	FMI
2	Vindeln	64.24	19.77	225	Brewer MKII 006	SMHI
3	Jokioinen	60.82	23.50	106	Brewer MKIII 107	FMI
4	Oslo	59.90	10.73	50	Brewer MKV 042	U_Oslo
5	Churchill	58.74	−93.82	16	Brewer MKII 026, Brewer MKIV 032, Brewer MKIII 203	WOUDC
6	Norrköping	58.58	16.15	43	Brewer MKIII 128	SMHI
7	Copenhagen	55.63	12.67	50	Brewer MKIVe 082	DMI
8	Obninsk	55.10	36.60	100	Brewer MKII 044	IEM-SPA
9	Edmonton	53.55	−114.10	766	Brewer MKII 055, Brewer MKIV 022	WOUDC
10	Manchester	53.47	−2.23	76	Brewer MKIII 172	U_Manchester
11	Goose Bay	53.29	−60.39	39	Brewer MKII 018	WOUDC
12	Warsaw	52.17	20.97	107	Brewer MKIII 207	PAS-IGF
13	De Bilt	52.10	5.18	24	Brewer MKIII 189	KNMI
14	Belsk	51.84	20.79	180	Brewer MKII 064	PAS-IGF
15	Reading	51.44	−0.94	66	Brewer MKIV 075, Brewer MKII 126	U_Manchester
16	Uccle	50.80	4.36	100	Brewer MKII 016, Brewer MKIII 178	RMIB
17	Regina	50.20	−104.71	580	Brewer MKIII 111	WOUDC
18	Hradec Králové	50.18	15.84	285	Brewer MKIII 184	CHMI-HK
19	Saturna Island	48.78	−123.13	178	Brewer MKII 012	WOUDC
20	Hohenpeißenberg	47.80	11.01	985	Brewer MKII 010	DWD-MOHp
21	Davos	46.81	9.84	1590	Brewer MKIII 163	PMOD/WRC
22	Arosa	46.78	9.67	1840	Brewer MKII 040, Brewer MKIII 156	MeteoSwiss
23	Aosta	45.74	7.36	569	Brewer MKIV 066	ARPA-VDA
24	Toronto	43.78	−79.47	198	Brewer MKII 015	WOUDC
25	Kislovodsk	43.73	42.66	2070	Brewer MKII 043	RAS-IAP
26	Rome	41.90	12.52	75	Brewer MKIV 067	U_Rome
27	Thessaloniki	40.63	22.95	60	Brewer MKII 005	AUTH
28	Boulder	40.03	−105.53	2891	Brewer MKIV 146	NEUBrew
29	Athens	37.99	23.78	191	Brewer MKIV 001	BRFAA
30	Izaña	28.31	−16.50	2373	Brewer MKIII 157	AEMET
31	T'aipei	25.04	121.51	5	Brewer MKIII 129	WOUDC
32	Mauna Loa	19.54	−155.60	3397	Brewer MKIII 119	WOUDC

Daily sulfur dioxide (SO_2) columns were analysed in four bimonthly periods, namely August–September 2008, April–May 2010, June–July 2011 and September–October 2014; these include the volcanic eruptions of Kasatochi (2008), Eyjafjallajökull (2010), Nabro (2011) and Bárðarbunga (2014) respectively. For the case of Kasatochi, Eyjafjallajökull and Bárðarbunga, we analysed daily SO_2 columns at 30 sites (listed in Table 2), while for the case of Nabro, whose impact was mostly seen over low latitudes in the Northern Hemisphere (e.g. Bourassa et al., 2012), we analysed SO_2 columns at three low-latitude sites in the Northern Hemisphere, namely Izaña, Mauna Loa and T'aipei.

Only for the case of the Bárðarbunga eruption in 2014 were the columnar SO_2 measurements over Europe also compared with surface SO_2 measurements from ground-based European stations. The surface SO_2 data were obtained from the European Environment Agency database (AirBase; http://www.eea.europa.eu/data-and-maps/data/aqereporting-1#tab-european-data) covering the bimonthly period September–October 2014. Only rural background stations, i.e stations in classes 1–2 according to the Joly–Peuch classification methodology for surface sulfur dioxide (Joly and Peuch, 2012), located at a distance of less than 150 km from the nearest Brewer station, were used in the analysis. A total of seven stations in Europe (see Table 3)

Table 3. Rural AirBase stations analysed in this study (see text).

Station ID	Station name	Latitude	Longitude	Closest Brewer (within 150 km)
GB0583A	Middlesbrough	54.569	−1.221	Manchester
NL00444	De Zilk-Vogelaarsdreef	52.298	4.51	De Bilt
PL0105A	Parzniewice	51.291	19.517	Belsk
NL00133	Wijnandsrade-Opfergeltstraat	50.903	5.882	Uccle
GB0038R	Lullington Heath	50.794	0.181	Reading
CH0005R	Rigi	47.067	8.463	Arosa
CH0002R	Payerne	46.813	6.944	Aosta

fulfilled the above-mentioned criteria and were included in the current analysis. Observed data from the AirBase network were available in hourly resolution, from which we calculated daily surface SO_2 values. We note here that SO_2 in the troposphere over western Europe is very low (e.g. Zerefos et al., 2009; Wild, 2012), and therefore plumes from volcanic eruptions are easy to detect against a lower background level.

2.2 Satellite data

The columnar SO_2 records from remote-sensing spectrophotometers over Europe, Canada, USA and Taiwan were compared with space-borne measurements from (a) the OMI aboard the EOS (Earth Observing System)-Aura (e.g. Ialongo et al., 2015) satellite and (b) the GOME-2 aboard the MetOp-A (e.g. Rix et al., 2009) satellite. We use MetOp-A instead of MetOp-B because it covers a longer time period. Both OMI and GOME-2 satellite SO_2 data products were downloaded from the Aura Validation Data Center (AVDC) (available from http://avdc.gsfc.nasa.gov/index.php?site=_245276100). GOME-2 level-2 overpass data have been processed with the GOME Data Processor (GDP) version 4.7. We analysed station overpass data for the various midlatitude stations listed in Table 2 and for the low-latitude stations at Mauna Loa, Izaña and T'aipei. The available OMI version 1.2.0 overpass (collection 3) data analysed in this study include pixels within 50 km radius from the nearest Brewer site and is not affected by OMI row anomalies. The available GOME-2 level-2 overpass data include pixels within 100 km radius from the Brewer sites.

For the case of OMI, the SO_2 data are provided from October 2004 to the present. There are four SO_2 products: (1) the planetary boundary layer SO_2 column (PBL), corresponding to a centre of mass altitude (CMA) at 0.9 km; (2) the lower tropospheric SO_2 column (TRL) corresponding to CMA of 2.5 km; (3) the middle-tropospheric SO_2 column (TRM), usually produced by volcanic degassing, corresponding to CMA of 7.5 km; and (4) the upper-tropospheric and stratospheric SO_2 column (STL), usually produced by explosive volcanic eruptions, corresponding to CMA of 17 km. Details on OMI SO_2 columns can be found in various studies (Levelt et al., 2006; Yang et al., 2007; Fioletov et al., 2011, 2013; McLinden et al., 2012; Li et al., 2013; Ialongo et al., 2015). In this study, we made use of the product for the middle-tropospheric SO_2 column (TRM) following the recommendation that the TRM retrievals should be used for volcanic degassing at all altitudes because the PBL retrievals are restricted to optimal viewing conditions and TRL data are overestimated for high-altitude emissions (> 3 km) (Ialongo et al., 2015). Also, we analysed the STL data which are intended for use with explosive volcanic eruptions where the volcanic cloud is placed in the upper troposphere/stratosphere. The standard deviation of TRM retrievals in background areas is reported to be about 0.3 DU in low and midlatitudes and about 0.2 DU for the STL retrievals. This is similar to the standard deviations (indicative of typical uncertainties of the measurements) that we find for the TRM and STL retrievals in the four bimonthly periods under this study. For the best data quality, we used data from the scenes near the centre of the OMI swath (rows 4–54) as recommended by Ialongo et al. (2015), who found that data from the edges of the swath tend to have greater noise.

For GOME-2, we analysed the total SO_2 columns from April 2007 to the present. The standard deviation found in our study for the GOME-2 retrievals is on the order of 0.4 DU. We analysed satellite SO_2 measurements whenever the O_3 column was between 250 and 450 DU and the solar zenith angle was less than 73.5°. We used SO_2 data defined as having a cloud radiance fraction (across each pixel) of less than 50 %, as they were found to have a smaller standard deviation than all sky data. Moreover, a range of SO_2 values between −35 and 35 DU was used to screen for outliers. In cases of multiple daily data matched to the station overpass, all available measurements within a radius of 50 (100) km from the Brewer site in the case of OMI (GOME-2) are averaged.

Finally, both for the satellite and the Brewer data, we have considered that during a 10-day period prior to any eruption both the surface and the satellite datasets represent a baseline reference from which subsequent departures after the eruption should be tested as to their significance. Therefore, we calculated averages and standard deviations (σ) of departures from the unperturbed pre-volcanic period, for the three studied periods of volcanic importance at each station,

Table 4. SO_2 column departures at midlatitude stations averaged in bimonthly periods following volcanic eruptions.

		August–September 2008 (Kasatochi)		April–May 2010 (Eyjafjallajökull)		September–October 2014 (Bárðarbunga)	
(a)	latitude	mean	σ	mean	σ	mean	σ
Sodankylä	67.36	0.6	2.1	0.1	0.7	−0.5	1.8
Vindeln	64.24	0.4	1.4	0.0	0.4	−0.2	0.9
Jokioinen	60.82	0.5	0.6	*	*	0.4	0.5
Oslo	59.90	*	*	0.7	0.6	−0.1	1.0
Churchill	58.74	0.6	0.8	−0.3	1.1	0.4	1.0
Norrköping	58.58	0.4	0.8	−0.1	0.2	0.1	0.8
Copenhagen	55.63	0.3	0.8	0.5	0.9	−0.4	0.7
Obninsk	55.10	*	*	0.1	0.5	0.3	0.9
Edmonton	53.55	0.4	0.6	0.4	0.4	0.0	0.4
Manchester	53.47	0.6	0.7	0.0	0.6	0.4	1.6
Goose Bay	53.29	0.2	0.4	*	*	0.3	0.3
Warsaw	52.17	*	*	*	*	0.1	0.4
De Bilt	52.10	0.1	0.9	−0.3	0.9	0.2	0.8
Belsk	51.84	0.3	0.6	−0.4	0.4	0.4	0.5
Reading	51.44	0.2	0.7	1.2	1.2	0.3	1.7
Uccle	50.80	0.1	0.6	−0.5	0.6	0.7	1.3
Regina	50.20	0.0	0.9	*	*	*	*
Hradec Králové	50.18	0.2	0.4	−0.3	0.4	−0.6	0.7
Saturna Island	48.78	0.4	1.1	0.0	0.2	0.4	0.5
Hohenpeißenberg	47.80	0.0	0.5	0.5	0.6	−0.1	1.6
Davos	46.81	0.2	0.5	−0.1	0.3	−0.1	0.2
Arosa	46.78	0.6	1.5	−0.5	1.5	−0.1	0.5
Aosta	45.74	−0.1	0.6	0.0	0.6	−0.6	0.8
Toronto	43.78	0.5	1.0	−0.2	0.5	0.4	0.5
Kislovodsk	43.73	−0.3	0.3	−0.1	0.3	0.2	0.2
Rome	41.90	−0.1	1.1	−0.8	1.3	−0.2	0.5
Thessaloniki	40.63	0.4	0.7	−0.7	0.9	*	*
Boulder	40.03	0.1	0.5	0.1	0.9	*	*
Athens	37.99	0.9	0.8	−0.4	0.6	0.0	0.4
(b)		mean ± SE (N)		mean ± SE (N)		mean ± SE (N)	
All Brewers		0.29 ± 0.03 (1051)		−0.04 ± 0.03 (1064)		0.07 ± 0.03 (861)	
GOME-2		0.23 ± 0.02 (1057)		0.08 ± 0.01 (971)		−0.03 ± 0.02 (677)	
OMI (TRM)		0.15 ± 0.02 (741)		0.00 ± 0.02 (438)		0.01 ± 0.02 (395)	
OMI (STL)		0.12 ± 0.01 (741)		0.00 ± 0.01 (438)		0.01 ± 0.02 (395)	

SE: standard error. * Missing values are those possessing < 25 days of data in each bimonthly period or no data.

only if at least 25 daily values were available. The bimonthly averages for each station in the examined periods are presented in Table 4a. Table 4b shows the mean and standard error ($\sigma/\sqrt{N}$) of all bimonthly averages in each studied volcanic period. Averaging the departures from the pre-volcanic baseline for all Brewer stations and for all bimonthly periods gives a mean SO_2 columnar departure of 0.10 ± 0.03 DU. This estimate is on the same order of magnitude as the corresponding statistics for OMI (TRM) SO_2 column departures (0.05 ± 0.02 DU), OMI (STL) (0.04 ± 0.01 DU) and that measured by GOME-2 (0.09 ± 0.02 DU). The standard deviation of the bimonthly averages relative to their baselines, which was calculated from a large sample of data, was taken here as an approximation of the typical uncertainties in the columnar SO_2 measurements performed by the group of Brewers, OMI and GOME-2 instruments following volcanic eruptions.

2.3 Modelling tools

Dispersion of volcanic emissions is simulated with the Lagrangian transport model FLEXPART (FLEXible PARTicle dispersion model; Stohl et al., 2005; Brioude et al., 2013). The model is driven by hourly meteorological fields from the Weather Research and Forecasting (WRF) atmospheric model (Skamarock et al., 2008) at a horizontal resolution of 45 × 45 km. The initial and boundary conditions for the

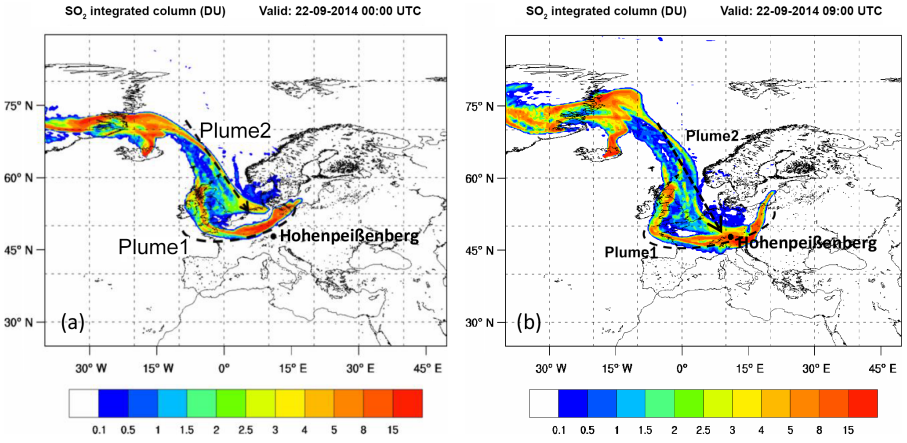

Figure 2. Integrated column of SO_2 (DU) from Bárðarbunga emissions as simulated with FLEXPART-WRF model, **(a)** 22 September 2014 00:00 UTC; **(b)** 22 September 09:00 UTC. Dashed lines indicate the orientation of the two distinct plumes overlapping over central Europe.

WRF model are taken from the National Center for Environmental Prediction (NCEP) final analysis (FNL) dataset at a $1° \times 1°$ resolution. The sea surface temperature (SST) is initialized from the NCEP $1° \times 1°$ analysis. A total of 40 000 tracer particles are assumed for each release in FLEXPART simulations. The use of 1-hourly WRF meteorological fields at a 45×45 km spatial resolution allows a more detailed representation of the volcanic plume dispersion but also implies a significant increase in computational time. To overcome this computational time cost, source–receptor relationships between station measurements and volcanic activity are also analysed with the use of HYSPLIT (Hybrid Single-Particle Lagrangian Integrated Trajectory) model trajectories (Stein et al., 2015) of long-range transport driven by the 3-hourly meteorological dataset Global Data Assimilation System (GDAS) at a resolution of $1° \times 1°$.

3 Results and discussion

3.1 The 2014 Bárðarbunga case

Bárðarbunga was continuously active during September–October 2014, but it was only during 18–26 September when meteorological conditions favoured transport towards Europe as shown by back trajectory analyses. A detailed description of the transport of Bárðarbunga plumes towards the station of Hohenpeißenberg is provided using the FLEXPART Lagrangian particle dispersion model offline coupled with the WRF_ARW atmospheric model. The simulation period is 18–26 September 2014. We assume a constant SO_2 release rate of 119 kilotons per day as reported by Gíslason et al. (2015) from near the source SO_2 measurements during the first weeks of the eruption. Similar emission rates are also suggested by Schmidt et al. (2015) through comparisons between NAME simulations (UK Met Office's Numerical Atmospheric-dispersion Modelling Environment) and OMI satellite retrievals. The emission height is set to between 0 and 3500 m above ground level, consistent throughout the simulation period. The establishment of an anticyclonic flow over the British Isles on 21 September 2014 (not shown here) resulted in the separation of the volcanic SO_2 field into two distinct plumes (Fig. 2a). On 22 September the primary plume (plume 1) becomes stagnant over the topographic barrier of the Alps (Fig. 2b). The secondary plume is advected southwards by the intense northerly winds over the North Sea. The two plumes overlap at about 09:00–11:00 UTC. Taking a closer look at the surface SO_2 values sampled during this event by surface air quality stations in the Netherlands, several days of enhanced SO_2 were discovered, which indicate an area of stagnation or blocking of the flow. Trajectory calculations performed at the Royal Netherlands Meteorological Institute (KNMI) correspond well to the calculations shown in Fig. 2 but also show that the air parcels stayed over northern Europe for some time after a very fast flow over the North Sea, which agrees with the spikes found in the surface SO_2 records observed over the Netherlands during a period of several days.

The high SO_2 concentrations, which were recorded almost simultaneously at stations over Europe at various sites during the period 21–29 September 2014, are thus associated with the activity of Bárðarbunga volcano (Ialongo et. al., 2015; Table A1, see Appendix A). This is also supported by the back trajectory analysis performed with the HYSPLIT dispersion model that is shown in Fig. 3. All back trajectories start at 12:00 UTC on the day of maximum SO_2 observations for each of the Brewer stations and indicate that the arrival of air masses originated from Iceland.

As shown in Fig. 4a, the SO_2 plume was detected by the Brewer instruments located in the passage of the volcanic SO_2 plume and from different ground-based networks. However, no coincident measurements were available from the OMI and GOME-2 overpasses at the time of the high SO_2 ex-

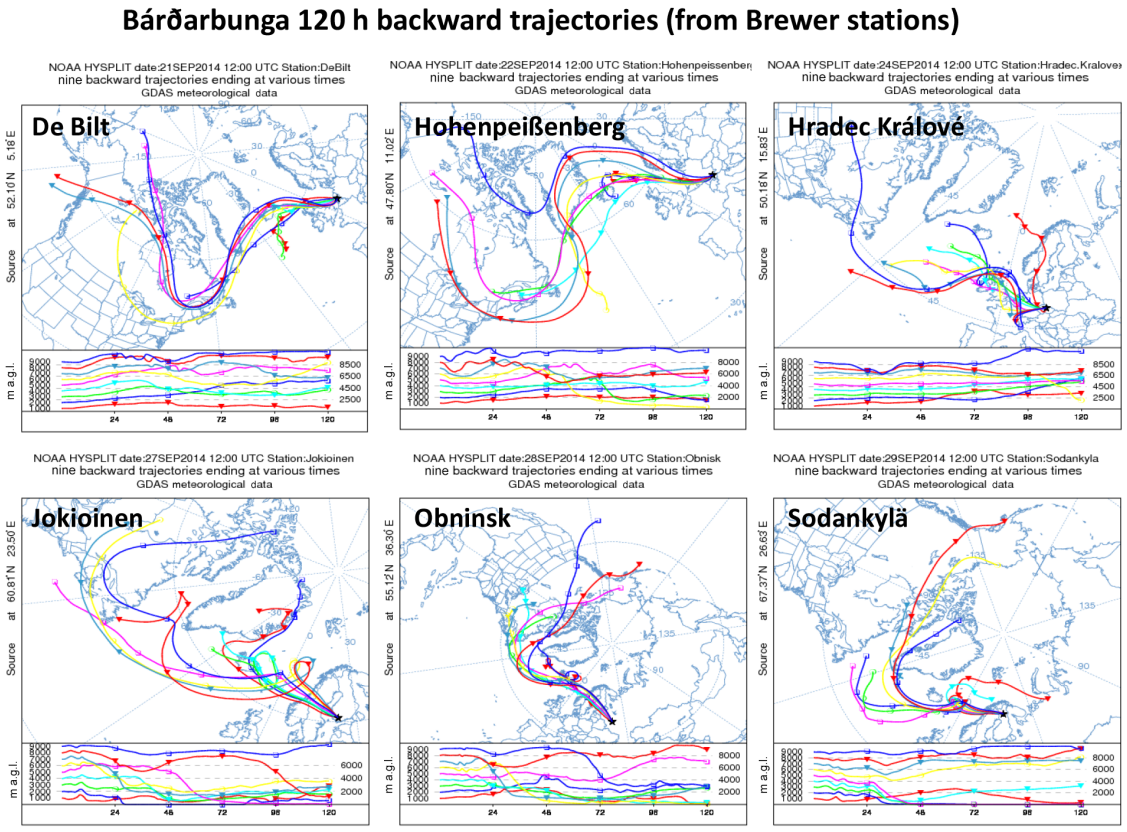

Figure 3. HYSPLIT 120 h back trajectories of air masses arriving on the day of maximum SO_2 records for each of the Brewer stations at De Bilt, Hohenpeißenberg, Hradec Králové, Jokioinen, Obninsk and Sodankylä.

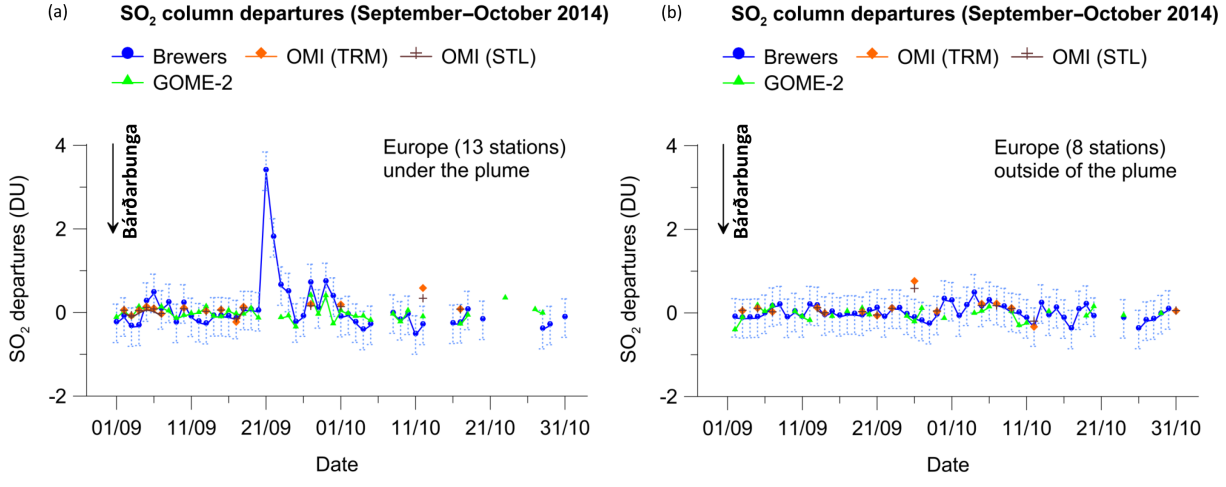

Figure 4. Mean SO_2 column departures from the unperturbed 10-day pre-volcanic baseline measured by Brewers, OMI (TRM, STL) and GOME-2 during September–October 2014 over Europe following the 2014 Bárðarbunga volcanic eruption for **(a)** stations under the volcanic SO_2 plume and **(b)** stations outside of the plume. The error bars for the Brewer observations show the standard deviation of all daily values during the unperturbed 10-day period prior to the volcanic eruption. Brewer stations under the plume are Sodankylä, Vindeln, Jokioinen, Oslo, Norrköping, Copenhagen, Obninsk, Manchester, De Bilt, Reading, Uccle, Hradec Králové, Hohenpeißenberg and Aosta. Stations outside of the plume are Warsaw, Belsk, Davos, Arosa, Kislovodsk, Rome and Athens. Each daily average from either OMI or GOME-2 was calculated if and only if more than half of the individual overpasses had data on a given day. The arrow marks the starting date of the eruption (beginning on 31 August 2014 and continuing to be active throughout the whole bimonthly period and beyond).

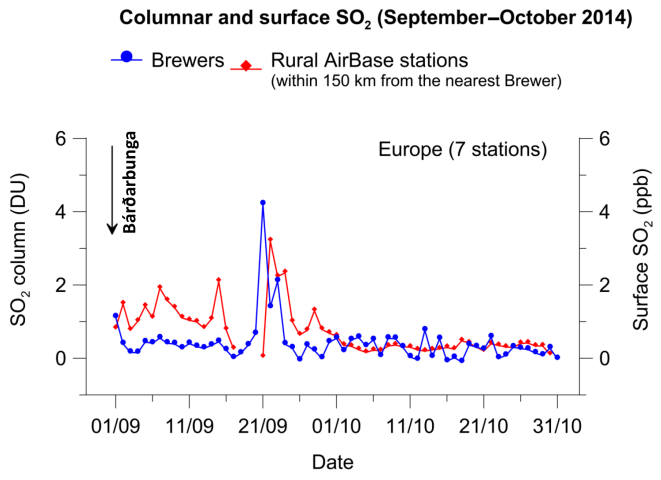

Figure 5. Mean surface SO_2 measured by AirBase class 1–2 stations located within 150 km from seven nearest Brewer stations in Europe as listed in Table 3. The arrow marks the starting date of the eruption (beginning on 31 August 2014 and continuing to be active throughout the whole bimonthly period and beyond).

cursions. Also it should be noted here that no enhanced SO_2 columns were detected by the Brewers located outside of the geographical area covered by the volcanic plume (Fig. 4b). In all volcanic cases we have applied a criterion according to which each daily average from either OMI or GOME-2 should be calculated if and only if more than half of the individual overpasses had data on a given day.

The eruption took place at the beginning of September 2014, and several European countries experienced high concentrations of SO_2 at ground level during the rest of September. Figure 5 shows the response of ground-level AirBase stations under the plume located within 150 km from the nearest Brewer station plotted together with the coincident Brewer SO_2 column measurements. Interestingly, it suggests that the highest amount of the SO_2 column measured by the majority of the Brewers on 21 September 2014 due to the volcano reached the surface with a time lag of about 1 day. The high volcanic concentrations were successfully measured by the ground-based AirBase network. Due to strong European efforts over the last decades to reduce SO_2 emissions, high concentrations of SO_2 are now quite rare in western Europe (e.g. Vestreng et al., 2007) except in the areas affected by industrial or shipping emissions. In situ air quality stations observed high values of SO_2 at the ground level on the coast of France, in the United Kingdom, the Netherlands and Germany between 21 and 25 September 2014. This all points towards a volcanic episode with a large spatial extent.

As can be seen from Fig. 4a, the highest SO_2 column departures from the pre-volcanic baseline were observed from 21 to 22 September 2014. The mean SO_2 column measured by the Brewers under the plume was 2.4 ± 0.8 DU, which was 5 times greater than the mean column of SO_2 measured by the Brewers outside of the plume (-0.1 ± 0.1 DU) by 2.5 DU on average. The error bars show the standard deviation of the daily SO_2 values of all stations during the non-perturbed 10-day period prior to the volcanic eruption. These differences provide rough estimates of the additional SO_2 loading induced by the volcanic eruption over Europe which exceeds 3σ. Comparison between satellite data and Brewer are limited for the purposes of interpretation because satellite measurements are sparse, representing an average SO_2 column over a relatively large satellite pixel, while the Brewer observations are designed to provide a local point measurement. In spite of the sparsity of OMI observations post Bárðarbunga volcanic eruption, satellite data were used for assimilation in the SO_2 analyses and forecasts produced with the MACC (Monitoring Atmospheric Composition and Climate) system (http://atmosphere.copernicus.eu/). This near-real-time forecasting system assimilates satellite observations to constrain modelling forecasts (Inness et al., 2015; Flemming et al., 2015). The OMI instrument aboard the Aura satellite provided information about concentrations of volcanic SO_2 emitted by the Icelandic Bárðarbunga volcano on 20 September; these observations were assimilated in 2014 by the MACC system in cases of volcanic eruptions, i.e. when OMI values exceeded 5 DU. As shown in Fig. 6 (the charts of total column SO_2 are taken from the website http://atmosphere.copernicus.eu/), the subsequent forecasts capture the transport of the plume of volcanic SO_2 southward, while spreading over the continent on 21 and 22 September. The plume stretched all the way from Finland through Poland, Germany and France to southern England. A parallel forecast, for which no OMI data were used (Fig. 6, right), did not show any elevated SO_2 values, confirming that "normal" emissions of SO_2 (including shipping and industrial activities) could not explain the observed situation.

Finally, it should be mentioned here that the thin aerosol layer that was detected by the PollyXT lidar (Engelmann et al., 2016) over Leipzig at around 2–3 km on 23 and 24 of September 2014 was mostly associated with volcanic ash advection (Fig. 7). A corresponding cluster analysis of all 155-hourly HYSPLIT back trajectories during this period and for the heights of the layer detected by the lidar ($\sim$ 2.5–3.5km) is shown in Fig. 8. The increased wind shear that is evident between these heights does not allow a robust characterization of the air masses. However, the source contribution of about 20 % from Icelandic air masses supports the volcanic origin of the detected plume. During volcanic eruptions, ash and SO_2 may be injected to different altitudes and may follow different trajectories for long-range transport. EARLINET lidars can provide alerts on volcanic ash dispersion over Europe, especially when the systems are employed with depolarization capabilities (e.g. Pappalardo et al., 2013). For the Brewer network capabilities and the Hohenpeißenberg station, Figs. 7 and 8 demonstrate that a similar approach can be applied to contribute towards an early warning synergistic tool, as evidenced in the Bárðarbunga case study. The role of

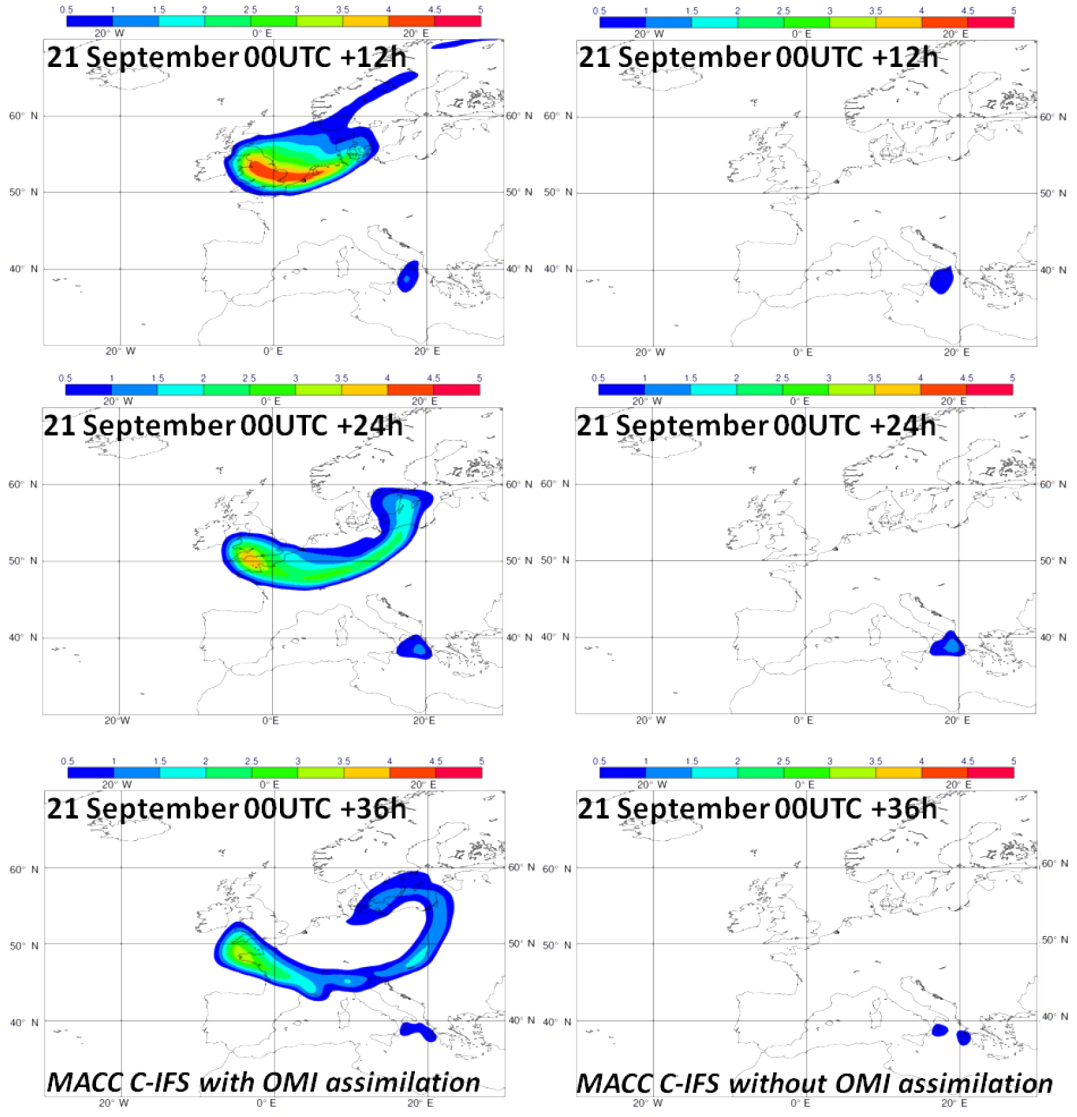

Figure 6. Charts of forecasted total column SO_2 produced within the MACC system for 21 September 2014 with OMI data assimilation (left) and without OMI data assimilation (right).

the Brewer stations in this system will be the early detection of SO_2 plumes transported over continental areas that would trigger the associated forecasting systems (models and networks).

3.2 The 2011 Nabro volcano plume

A major eruption of Mt Nabro, a 2218 m high volcano on the border between Eritrea and Ethiopia (13.37° N, 41.7° E), occurred on 12–13 June 2011. The volcanic eruption injected ash, water vapour and an estimated 1.3–2.0 Tg of SO_2 into the upper troposphere and lower stratosphere (Fairlie et al., 2014, and references therein). In the first phase of the eruption, the main transport pattern of emitted SO_2 followed the strong anticyclonic circulation over the Middle East and Asia associated with the Asian summer monsoon at that time of year (Clarisse et al., 2014, and references therein). In the first month after the eruption stratospheric aerosols were mainly observed over Asia and the Middle East and by day 60 covered the whole Northern Hemisphere. Estimated aerosol altitudes from various instruments were between 12 and 21 km (Clarisse et al., 2014). By July 2011 Nabro had cumulatively emitted 5 to 10 % of what was released by Mount Pinatubo in 1991 ($\sim$ 20 Tg), ranking it among the largest SO_2 emissions in the tropical stratosphere (up to at least 19 km) since Pinatubo (Krotkov et al., 2011). Sulfur dioxide signals of volcanic origin were detected both by Brewer and satellite measurements over East Asia, where the volcanic SO_2 plume was transported, as demonstrated in Figs. 9 and 10a. Measurements were taken by Brewer in T'aipei, Taiwan, Asia. This is also evident from the back trajectory analysis performed

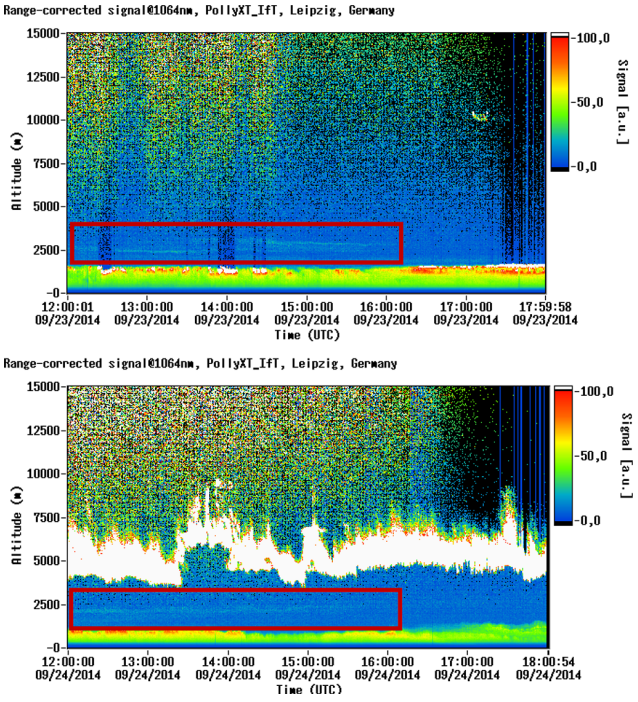

Figure 7. Range-corrected signal at 1064 nm from the PollyXT lidar in Leipzig on 23 (up) and 24 September 2014 (down). The red rectangle indicates the location of the volcanic ash layer.

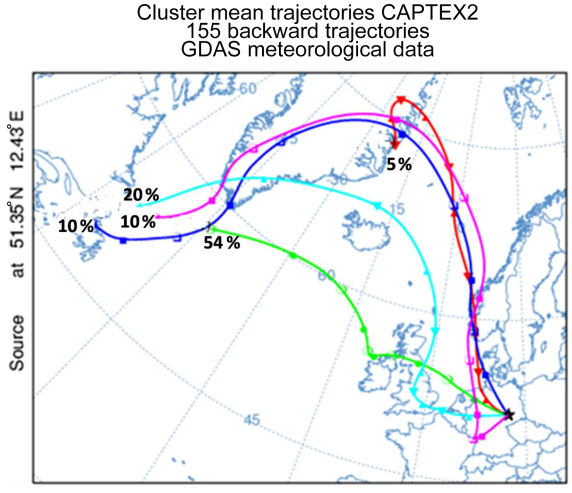

Figure 8. Cluster analysis of the HYSPLIT back trajectories that arrive every hour (from 23 September 12:00 UTC up to 24 September 18:00 UTC) at 2.5–3.5 km height over Leipzig. A 54 % cluster percentage means that there is 54 % chance that the SO_2 arriving anywhere between 2.5 and 3.5 km over Leipzig originates from the specific direction.

with the HYSPLIT dispersion model for T'aipei (Taiwan) as shown in Fig. 10a. The analysis indicates that the upper-tropospheric air masses arriving at T'aipei on 19 June, when the peak in SO_2 is observed, originate from Africa.

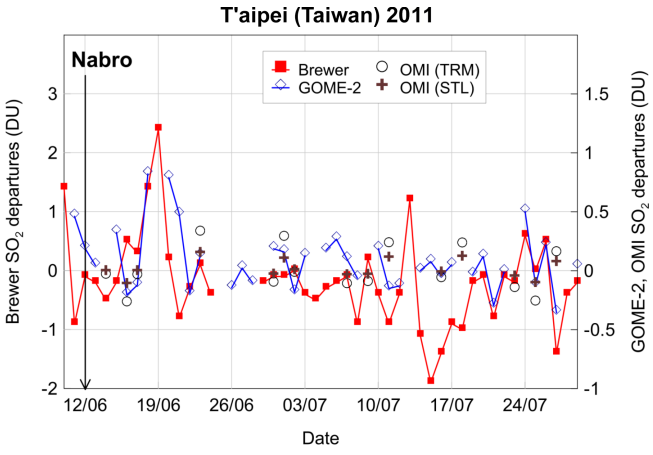

Figure 9. SO_2 column departures from the unperturbed 10-day pre-volcanic baseline measured by Brewer, OMI (TRM, STL) and GOME-2 over T'aipei, Taiwan, during June–July 2011 following the 2011 Nabro volcanic eruption (on 12 June 2011).

The Nabro volcanic plume was mainly transported to East Asia and was detected by various satellite instruments which provide better spatial coverage than the Brewers. A special case study focuses on discrepancies found between ground-based and satellite observations of the volcanic SO_2 plume. A Brewer located in Tenerife, Spain, detected an increase in the SO_2 column, which was not clearly detected by the OMI and GOME-2 satellite overpasses.

More specifically, Fig. 10b shows back trajectories from Izaña (Tenerife) during 19–29 June 2011 at 15, 17.5 and 20 km heights. It appears that the upper-tropospheric–lower-stratospheric air masses arriving at Tenerife during 19–29 June originated from Nabro. In June 2011 the Nabro volcano ash plume was detected by the Micropulse Lidar (MPL) located at Santa Cruz de Tenerife (Canary Islands, Spain). The volcanic plume height ranged from 12 km on 19 June to 21 km on 29 June (Sawamura et al., 2012). Figure 11 shows the columnar SO_2 departures from the unperturbed 10-day pre-volcanic baseline measured by the Brewer at Izaña following Nabro. The daily mean SO_2 departures (Fig. 11) show a 0.3 DU increase at the beginning of the event (19 June), reaching 0.6 DU on 29 June when the layer is found at a higher altitude. The signal is not strong and is near the error of 0.5 DU estimated for SO_2 measurement (Stanek, personal communication, 2016), but the observations are consistent (independent of the ozone and air mass), since at Izaña about 100 O_3/SO_2 measurements per day are performed resulting in reduced standard errors associated with daily means as compared to individual observations. The Langley calibration is tracked between calibrations by measurements of the internal lamp (Langley and lamp are shown in Supplement Fig. S1). The increase in SO_2 due to the passage of the Nabro volcano plume over the Canary Islands is significant using both methods (Fig. 11).

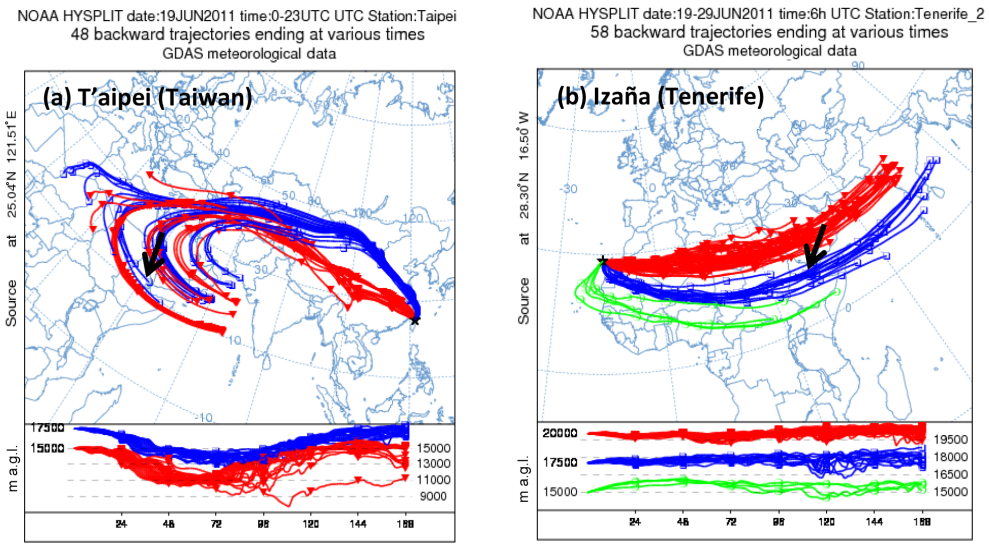

Figure 10. HYSPLIT back trajectories of air masses **(a)** from T'aipei (Taiwan) on 19 June 2011 and **(b)** from Izaña (Tenerife) for days 19–29 June 2011. Nabro's location is indicated by the black arrow.

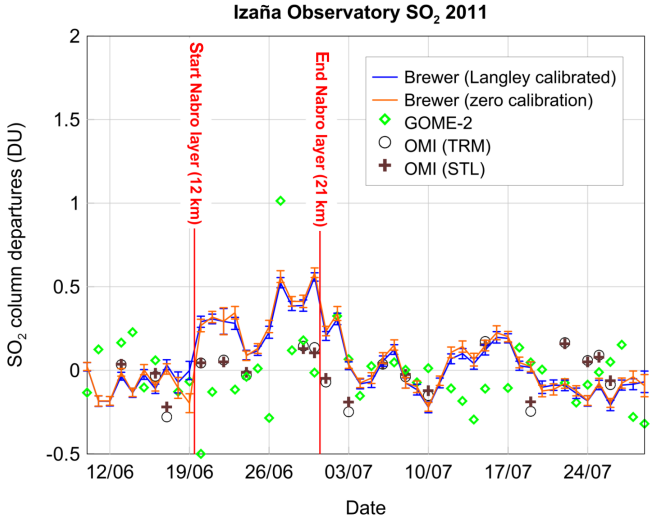

Figure 11. SO_2 column departures from the unperturbed 10-day pre-volcanic baseline measured by the Brewer, OMI (TRM, STL) and GOME-2 over Izaña, Tenerife, during June–July 2011 following the 2011 Nabro volcanic eruption. SO_2 calculations by the Brewer were performed using the Langley calibration and the zero calibration at Izaña (assuming $SO_2 = 0$ during the days 6 and 7 June 2011).

In this case the Brewer at Izaña has been able to detect an SO_2 plume at a high altitude from a volcano located 7000 km from the Canary Islands, indicating that the Brewer network is sensitive enough to be incorporated into columnar SO_2 monitoring from volcanic eruptions in worldwide networks.

The case of the 2011 Nabro eruption shows an example of the importance of the Brewer spectrophotometers in measuring and detecting changes in SO_2 amounts in the atmosphere due to volcanic eruptions, in cases where signal in the satellite overpasses is low. This is true for the case of Izaña (Tenerife), where it appears that OMI and GOME-2 did not clearly detect increases in SO_2 column of volcanic origin between 19 June and 1 July as was the case with the Brewer instrument (Fig. 11). During some days between 19 June and 1 July, the Brewer SO_2 columns at Izaña rose above the uncertainty of 0.5 DU for the Brewer SO_2 measurements at this station, whereas the satellite SO_2 columns stayed mostly within the uncertainty of 0.4 DU estimated for OMI and GOME-2 satellite retrievals.

These findings can provide clues to the detection limits of such events from a well-calibrated Brewer network and a space-borne instrument. They need further clarification with more Brewers and a larger number of cases.

3.3 The case of the 2010 Eyjafjallajökull volcanic eruption

The Eyjafjallajökull volcano, Iceland (63.63° N, 19.6215° W; 1666 m a.s.l.), erupted explosively on 14 April 2010 and continued to emit ash and gas until 24 May (Flentje et al., 2010; Thomas and Prata, 2011; Stohl et al., 2011; Flemming and Inness, 2013). Despite the relatively modest size of the eruption, the prevailing wind conditions advected the volcanic plume toward the southeast leading to unprecedented disruption to air traffic in western Europe. This caused significant financial losses for the airlines and highlights the importance of efficient volcanic cloud monitoring and forecasting. Results demonstrate that the eruption can be divided into an initial ash-rich phase (14–18 April), a lower-intensity middle phase (19 April until early May) and a final phase (4–24 May), where

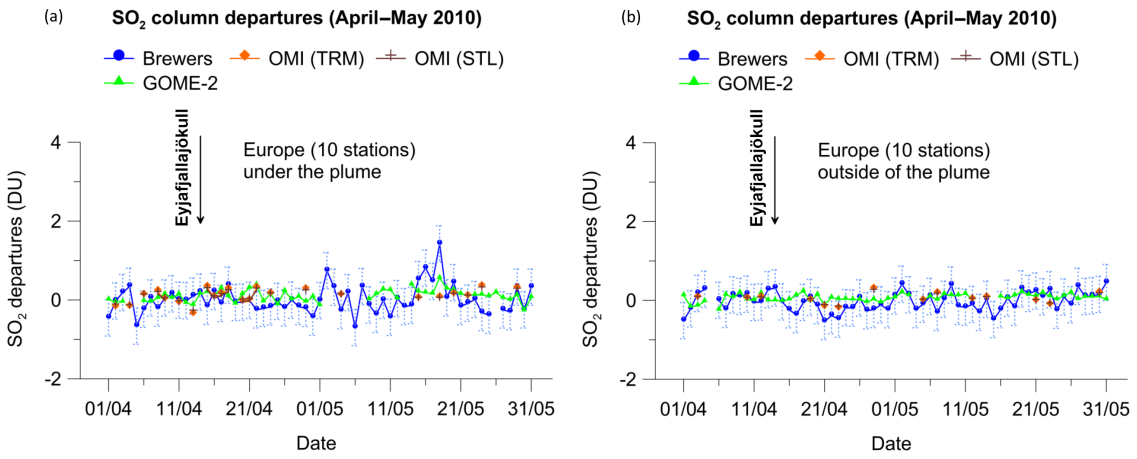

Figure 12. Mean SO_2 column departures from the unperturbed 10-day pre-volcanic baseline measured by Brewers, OMI (TRM, STL) and GOME-2 during April–May 2010 over Europe following the 2010 Eyjafjallajökull volcanic eruption for **(a)** stations under the volcanic SO_2 plume and **(b)** stations outside of the plume. The error bars for the Brewer observations show the standard deviation of all daily values during the unperturbed 10-day period prior to the volcanic eruption. Brewer stations under the plume are Sodankylä, Obninsk, Manchester, De Bilt, Uccle, Belsk, Reading, Hohenpeißenberg, Davos and Arosa. Stations outside of the plume are Vindeln, Oslo, Norrköping, Copenhagen, Hradec Králové, Aosta, Kislovodsk, Rome, Thessaloniki and Athens. Each daily average from either OMI or GOME-2 was calculated if and only if more than half of the individual overpasses had data on a given day. The arrow marks the starting date of the eruption (beginning on 14 April until 24 May 2010).

considerably greater quantities of both ash and SO_2 were released (Thomas and Prata, 2011).

Figure 12 shows the responses of Brewer stations under the volcanic SO_2 plume and the average of Brewer stations outside of the plume together with OMI and GOME-2 satellite observations. We determined 10 stations as being under the plume in 2010 and 10 stations as being outside of the plume based on the analysis of forward and backward trajectories of air masses following the volcanic eruption. The stations determined to be under the plume in 2010 (shown in Fig. 12a) are Sodankylä, Obninsk, Manchester, De Bilt, Uccle, Belsk, Reading, Hohenpeißenberg, Davos and Arosa. The stations determined to be outside of the plume are Vindeln, Oslo, Norrköping, Copenhagen, Hradec Králové, Aosta, Kislovodsk, Rome, Thessaloniki and Athens (Fig. 12b).

We should note here that volcanic clouds can be rather narrow plumes with diameters on the order of a few tens of kilometres (e.g. Stohl et al., 2011; Webley et al., 2012; Thorsteinsson et al., 2012; Kristiansen et al., 2012; Kokkalis et al., 2013), and thus it is possible that a volcanic layer detected at a specific station is not observed by neighbouring stations. The measurements at Uccle and De Bilt that are located at a horizontal distance of 150 km are different during the Eyjafjallajökull episode and provide a very good example. On 2 May 2010 the mean daily SO_2 is 5.8 DU at De Bilt and −0.2 DU at Uccle. As seen in the corresponding back trajectories for that day in Fig. 13, air masses originating from Iceland arrive at De Bilt at heights of 6–7 km and have probably transported the volcanic cloud over that station. In contrast similar back trajectories on the same day for the case of Uccle indicate transport of air masses from Iceland but at lower heights (3–4 km) that were probably not affected by the volcanic emissions. In another case of transport on 11 May 2010, Uccle was outside of the plume (see Fig. 13), while the mean daily SO_2 for De Bilt was 0.9 DU. On 18 May 2010, both De Bilt and Uccle stations detected a volcanic cloud with SO_2 daily means of 1.7 and 1.2 DU respectively. To summarize, in spite of the proximity of Uccle and De Bilt, the transport heights and trajectories can have a different result in transporting volcanic gases.

In Table A1 of Appendix A, we present the dates when the examined Brewer stations were either under or outside of the volcanic SO_2 plume. Careful analysis of the trajectories of the volcanic plumes in 2010 and 2014 helped verify these analyses. The distinction between stations outside of the plume and stations under the plume was done as follows: whenever SO_2 at each station measuring exceeded 2 DU (2σ), back trajectories were calculated and the origin was compared to the location of the volcanic eruption. All these stations have been considered to be under the SO_2 plume. All other stations, for which columnar SO_2 amounts were within 2σ and did not originate from the area of the eruption, were considered to be outside of the volcanic SO_2 plume.

As we can see from Fig. 12, the columnar SO_2 departures at stations located under the passage of the volcanic SO_2 plume exceeded 0.3 DU (reaching 1.5 DU in some cases), whereas at stations located outside of the plume, the columnar SO_2 departures did not exceed 0.3 DU. Moreover, during the explosive phase 2, there were three main periods in

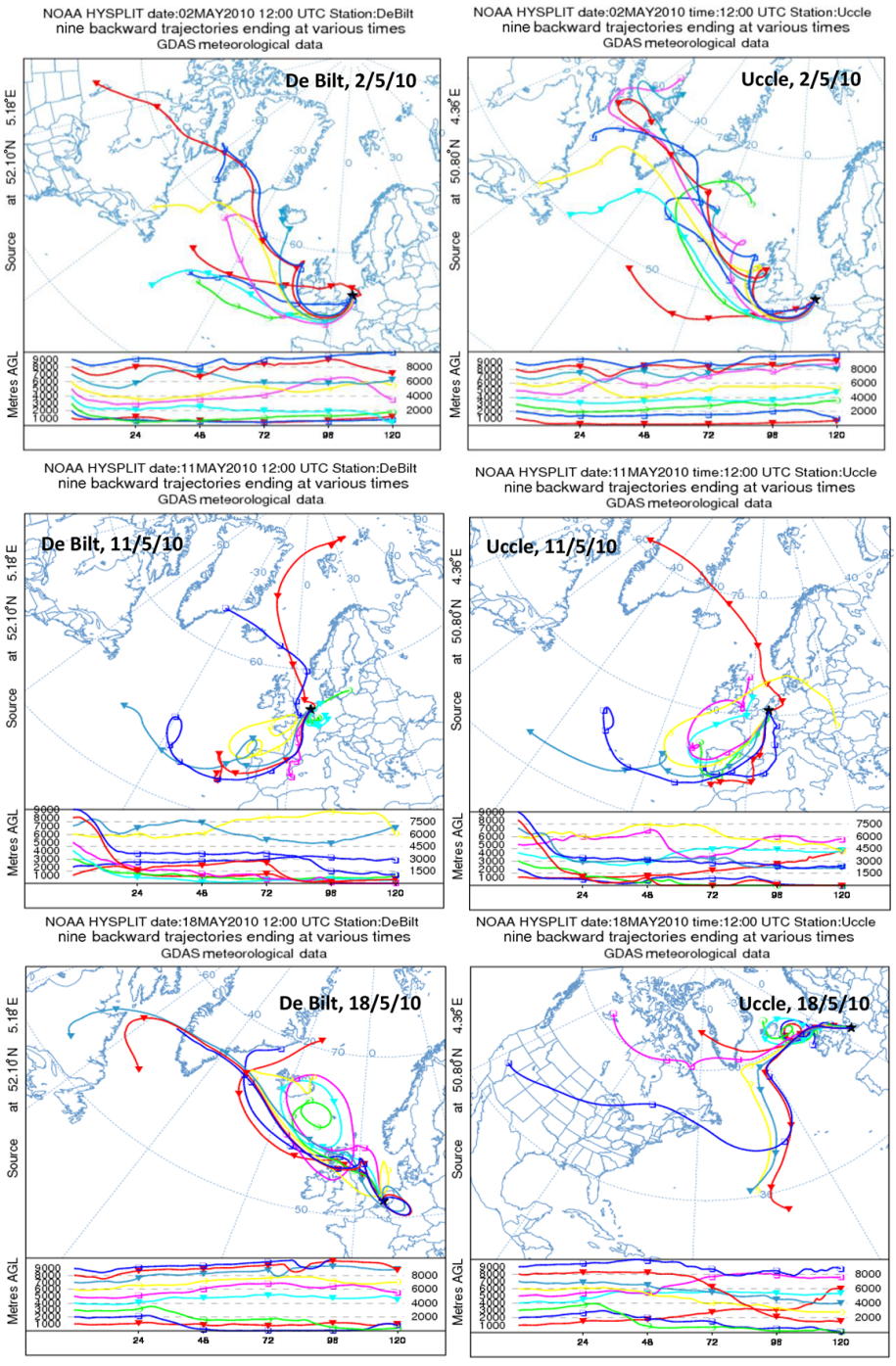

Figure 13. HYSPLIT 120 h back trajectories of air masses arriving at De Bilt (left column) and Uccle (right column) on 2 May 2010 (first row), 11 May 2010 (second row) and 18 May 2010 (third row).

which the volcanic aerosol content was observed by EARLINET over Europe: 15–26 April, 5–13 May and 17–20 May. These periods were determined from measurements of the integrated backscatter at 532 nm in the volcanic layers (Pappalardo et al., 2013). We estimate high SO_2 columnar departures measured by the Brewers under the plume during 14 April and 23 May 2010 of up to 6.0 DU (e.g. Arosa, 18 May 2016).

We note here that the ash cloud caused further disruptions to air transportation on 4–5 May and 16–17 May 2010, particularly over Ireland and the UK. The average SO_2 columnar departures measured by the Brewers under the plume in the

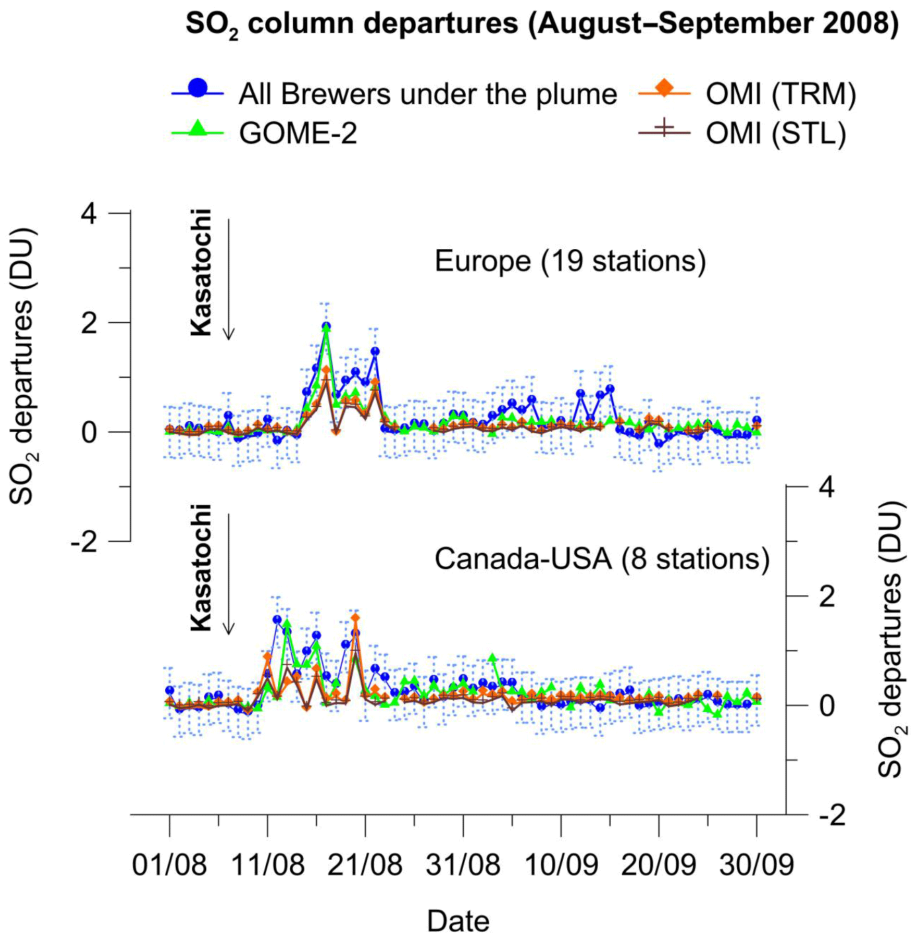

Figure 14. Mean SO_2 column departures from the unperturbed 10-day pre-volcanic baseline measured by Brewers, OMI (TRM, STL) and GOME-2 during August–September 2008 over Europe and Canada and the USA following the 2008 Kasatochi volcanic eruption. The error bars for the Brewer observations show the standard deviation of all daily values during the unperturbed 10-day period prior to the volcanic eruption. Stations in Europe include Sodankylä, Vindeln, Jokioinen, Norrköping, Copenhagen, Manchester, De Bilt, Belsk, Reading, Uccle, Hradec Králové, Hohenpeißenberg, Davos, Arosa, Aosta, Kislovodsk, Rome, Thessaloniki and Athens. Stations in Canada and the USA include Churchill, Edmonton, Goose Bay, Regina, Saturna Island, Toronto, Boulder and Mauna Loa. Each daily average from either OMI or GOME-2 was calculated if and only if more than half of the individual overpasses had data on a given day. The arrow marks the date of the eruption (7 August 2008).

UK (Manchester and Reading) during these two periods were estimated to 1.1 ± 0.3 and 1.5 ± 0.4 DU respectively. These amounts were higher than the amounts measured outside of the plume (-0.1 ± 0.2 and -0.1 ± 0.1 DU, accordingly) by almost 1.4 DU on average.

3.4 An eruption of larger-scale importance – the 2008 Kasatochi case

The eruption of Kasatochi volcano on 7–8 August 2008 injected large amounts of material and SO_2 into the troposphere and lower stratosphere of the northern middle latitudes during a period of low stratospheric aerosol background concentrations. The Kasatochi volcano in the central Aleutian Islands of Alaska (52.17° N, 175.51° W) erupted three times between 22:01 UTC on 7 August and 04:35 UTC on 8 August 2008 (Bitar et al., 2010). Aerosols from the volcanic eruption were detected by lidar in Halifax shortly after the eruption (Bitar et al., 2010). The total mass of SO_2 injected into the atmosphere by the eruption is estimated at 1.7 Tg, with about 1 Tg reaching the stratosphere (above 10 km a.s.l.) (Kristiansen et al., 2010).

We have studied the columnar SO_2 amounts following the Kasatochi eruption in August 2008 from ground-based and satellite data. Figure 14 shows the columnar SO_2 departures from the unperturbed 10-day pre-volcanic period over Canada and the USA and Europe during the bimonthly period August–September 2008 as measured by the Brewers in comparison with the satellite observations by OMI and GOME-2.

Table 5. Correlation coefficients between the mean columnar SO_2 measured by the Brewers in Europe and provided by the satellite products of OMI and GOME-2 during the volcanic eruptions of Kasatochi (2008), Eyjafjallajökull (2011) and Bárðarbunga (2014) for stations located under the volcanic SO_2 plume.

Europe	August–September 2008	April–May 2010	September–October 2014
Brewers and GOME-2	**0.86** [59] ($p < 0.0001$)	**0.31** [54] ($p = 0.02336$)	**0.44** [39] ($p = 0.00496$)
Brewers and OMI (TRM)	**0.86** [50] ($p < 0.0001$)	(*) [23]	(*) [15]
Brewers and OMI (STL)	**0.86** [50] ($p < 0.0001$)	(*) [23]	(*) [15]
GOME-2 and OMI (TRM)	**0.92** [48] ($p < 0.0001$)	(*) [21]	(*) [15]
GOME-2 and OMI (STL)	**0.93** [48] ($p < 0.0001$)	(*) [21]	(*) [15]

Bold: all the above correlations are significant at confidence level 95 % or greater (t test). * Missing correlations are those possessing less than 30 days of data in each bimonthly period. In square brackets: number of pairs.

The SO_2 plume was clearly seen by the Brewers in Canada and the USA (Fig. 14), and it was also detected by the majority of the Brewers in Europe with a delay of about 3 days. The total SO_2 columnar departures averaged over Canada during the period 12–20 August 2008 are estimated to 0.9 ± 0.2 DU. Accordingly over Europe, we estimate a mean SO_2 columnar departure of 1.0 ± 0.1 DU during the period 15–22 August 2008. This number gives a rough estimate of the average volcanic SO_2 column measured by the Brewers over Europe. We note here that the e-folding time of the Kasatochi SO_2, i.e. the time where the volcanic SO_2 amount decayed, was estimated to be about 8–9 days (Krotkov et al., 2010).

The high amounts of SO_2 and the variability of SO_2 measured in Europe by the Brewers after the eruption of Kasatochi in August 2008 are in line with OMI and GOME-2 satellite observations. More specifically, OMI (TRM) shows an average SO_2 columnar departure of 0.5 ± 0.1 DU during the period 15–22 August 2008, OMI (STL) an average SO_2 columnar departure of 0.4 ± 0.1 DU and GOME-2 an average SO_2 columnar departure of 0.8 ± 0.1 DU.

The Brewer data have been correlated with those from OMI and GOME-2. The Pearson's correlation coefficients between the three datasets were all highly statistically significant (> 99 %). The correlation between SO_2 from the Brewers and SO_2 from GOME-2 at 19 stations averaged over Europe is +0.86 (t value = 12.54; p value < 0.0001; $N = 59$). Accordingly, the correlation between Brewer and OMI (TRM) SO_2 data is +0.86 (t value = 11.77; $p < 0.0001$; $N = 50$), and between GOME-2 and OMI (TRM) data, it is +0.92 (t value = 16.32, $p < 0.0001$, $N = 48$). The same correlations are found for the Brewer–OMI (STL) and GOME–OMI (STL) data pairs. These correlations were calculated from 60 daily averages during the Kasatochi volcanic eruption in August–September 2008. The statistical tests gave significant results and verified the capability of the Brewers in detecting natural SO_2 emitted by volcanoes when the volcanic plume of SO_2 passes over the ground sites. We note here that there is a general consistency between all three datasets (Brewers, OMI and GOME-2) on the changes in SO_2 column following the Kasatochi volcanic eruption.

Table 5 summarizes the correlation coefficients between the mean columnar SO_2 measured by all Brewers over Europe and provided by the satellite products of OMI and GOME-2 during the globally extended Kasatochi event. The correlation coefficients have high statistical significance explaining more than 70 % of the total variance between the columnar SO_2 measurements from the ground and space in the case of Kasatochi. However, the discrepancies found between satellite and Brewer observations during the other volcanic eruptions could be impacted by the sparsity of coincident measurements and thus cannot confirm or deny Kasatochi case findings at high significance levels.

4 Conclusions

In this work we provide evidence that the current network of Brewer spectroradiometers is capable of identifying columnar SO_2 plumes of volcanic origin. The study is based on the results from the three largest volcanic eruptions (VEI ≥ 4) in the past decade when elevated SO_2 plumes have passed over Brewer stations in the Northern Hemisphere. The analysis included a fourth eruption, namely Bárðarbunga, because it perturbed the SO_2 regime over large parts of Europe and extended from the free troposphere down to the surface. Back and forward trajectory analysis have been used to aid identifying and selecting measurements taken under and outside of the volcanic SO_2 plume. When the plume was passing over a site, the SO_2 signal was found to be quite high, exceeding 3σ of daily values relative to the average levels taken during the unperturbed measurements over 10 days preceding each eruption. On average, the mean SO_2 columnar amount to be attributed to the volcano is estimated to be on the order of 2 DU as discussed in Sect. 3. In addition to the Brewer network, comparisons were made with other instruments (e.g. surface SO_2 sensors) that were located under the volcanic SO_2 plumes. Moreover, satellite measurements of columnar SO_2 from OMI and GOME-2 collocated with the Brewer network were used for comparisons.

From the results discussed in Sect. 3 some general remarks can be put forward concerning SO_2 levels and detection time

after the eruption. Starting with the Kasatochi eruption, as it appears from Fig. 14, the plume can be detected 4 days after the eruption over Canada and the US and about 7 days over Europe with an average amplitude on the order of 2 DU compared to the unperturbed 10-day pre-volcanic period (baseline). All estimates are based obviously on measurements taken under the plume. The Kasatochi eruption provided a very good example for a volcanic SO_2 plume to be observed not only by the ground-based instruments but by space-borne ones as well (OMI and GOME-2). Relative to the undisturbed period before Kasatochi, the amplitude of the signal is 2 DU for GOME-2 and 1.5 DU for OMI. The results for the other volcanic eruptions are similar for the Brewer network, but unfortunately because of the sparsity of satellites passing over the Brewer stations, the satellite data concur with those from the Brewers only in Kasatochi. Based on the above discussion, it appears that currently no single network can independently and fully monitor the evolution of volcanic SO_2 plumes. Among a few reasons are a lack of measurements during peak values, complications from meteorological events, ejection heights and exposure conditions. The evidence presented here suggests that a combination of observations from various instruments, aided by chemical transport models and operated in synergy, could address such a complex issue.

The combination of the observation discussed above and modelling tools can assist in detecting existing volcanic plumes but also in forecasting their evolution, which can have importance not only for air traffic warnings but also for air pollution in the lower layers of the atmosphere. Therefore, an automated source–receptor modelling tool could be proposed as follows: a modelling system based on FLEXPART and HYSPLIT backward-trajectory simulations could be automatically triggered whenever high SO_2 values are detected at a Brewer station above a specific threshold (e.g. 3σ of station's daily values) or when a lidar instrument detects highly depolarizing layers that were not advected from a geographical location over a desert. The operational use of such synergistic activity could provide near-real-time and forecasting information on the evolution of volcanic episodes and also develop a comprehensive database of measurements useful to improve model forecasts. This new well-tuned and organized synergistic activity of monitoring networks, observations and modelling from the ground and space could create a promising monitoring tool for volcanic and other extreme emissions, which would form the basis of a new regional SO_2 columnar forecasting facility.

5 Data availability

SO_2 columns at Churchill, Goose, Edmonton, Regina, Saturna Island and Toronto in Canada, T'aipei in Taiwan, and Boulder and Mauna Loa in the US were obtained from the World Ozone and Ultraviolet Radiation Data Centre (WOUDC; http://www.woudc.org/; last access: 10 October 2016) and the NOAA-EPA Brewer Spectrophotometer UV and Ozone Network (NEUBrew; http://www.esrl.noaa.gov/gmd/grad/neubrew/; last access: 10 October 2016). OMI and GOME-2 satellite SO_2 data products were downloaded from the Aura Validation Data Center (AVDC) (available from http://avdc.gsfc.nasa.gov/index.php?site=_245276100; last access: 10 October 2016). Surface SO_2 concentrations over Europe were acquired from the European Environment Agency databases (AirBase) (http://www.eea.europa.eu/data-and-maps/data/aqereporting-1#tab-european-data; last access: 10 October 2016).

Appendix A

Table A1. Dates at which the Brewers were determined to be under or outside of the volcanic SO_2 plume, based on analysis of back trajectories of the volcanic plumes in 2010 and 2014. The distinction between stations outside of the plume and stations under the plume was done as follows: at each station measuring SO_2 exceeding 2 DU (2σ), we calculated back trajectories and found that their origin was at the volcanic eruption. All these stations have been considered to be under the SO_2 plume. All other stations, for which columnar SO_2 amounts were within 2σ and did not originate from the area of the eruption, were considered to be outside of the volcanic SO_2 plume. During the Kasatochi eruption all Brewers were considered to be under the volcanic SO_2 plume.

Station	Lat (deg)	Long (deg)	Alt (m)	2010	2014
Sodankylä	67.36	26.63	180	20 Apr	27 and 29 Sep
Vindeln	64.24	19.77	225	Outside the plume	29 Sep
Jokioinen	60.82	23.50	106	No data	27 Sep
Oslo	59.90	10.73	50	Outside the plume	Outside the plume
Norrköping	58.58	16.15	43	Outside the plume	30 Sep
Copenhagen	55.63	12.67	50	Outside the plume	24 Sep
Obninsk	55.10	36.60	100	23 and 25 Apr	28 Sep
Manchester	53.47	−2.23	76	16 May	21 Sep
Warsaw	52.17	20.97	107	No data	Outside the plume
De Bilt	52.10	5.18	24	2, 11, 18 May	21 Sep
Belsk	51.84	20.79	180	10 May	Outside the plume
Reading	51.44	−0.94	66	16 May	21 Sep
Uccle	50.80	4.36	100	18 May	21–22 Sep
Hradec Králové	50.18	15.84	285	Outside the plume	24 Sep
Hohenpeißenberg	47.80	11.01	985	18 May	22 Sep
Davos	46.81	9.84	1590	27 Apr and 18–19 May	Outside the plume
Arosa	46.78	9.67	1840	18 May	Outside the plume
Aosta	45.74	7.36	569	Outside the plume	23 Sep
Kislovodsk	43.73	42.66	2070	Outside the plume	Outside the plume
Rome	41.90	12.52	75	Outside the plume	Outside the plume
Thessaloniki	40.63	22.95	60	Outside the plume	No data
Athens	37.99	23.78	191	Outside the plume	Outside the plume

Acknowledgements. The authors would like to particularly thank Andreas Engel and two anonymous reviewers for their valuable comments. This research was supported by the Copernicus Atmosphere Monitoring Service (CAMS), the Mariolopoulos-Kanaginis Foundation for the Environmental Sciences and the project of EUMETSAT, O3M SAF. We acknowledge the COST Action ES1207 "A European Brewer Network (EUBREWNET)", the WMO World Ozone and Ultraviolet Radiation Data Centre (WOUDC), the NOAA-EPA Brewer Spectrophotometer UV and Ozone Network (NEUBrew), the NASA GSFC Aura Validation Data Center (AVDC) and the EEA European air quality database (AirBase).

This project has received funding from the European Union's Horizon 2020 research and innovation programme under grant agreement no. 654109.

Edited by: A. Engel
Reviewed by: two anonymous referees

References

Bais, A. F., Zerefos, C. S., Meleti, C., Ziomas, I. C., and Tourpali, K.: Spectral measurements of solar UVB radiation and its relation to total ozone, SO_2 and clouds, J. Geophys. Res., 98, 5199–5204, 1993.

Bitar, L., Duck, T. J., Kristiansen, N. I., Stohl, A., and Beauchamp, S.: Lidar observations of Kasatochi volcano aerosols in the troposphere and stratosphere, J. Geophys. Res., 115, D00L13, doi:10.1029/2009JD013650, 2010.

Bourassa, A. E., Robock, A., Randel, W. J., Deshler, T., Rieger, L. A., Lloyd, N. D., Llewellyn, E. J., and Degenstein, D. A.: Large Volcanic Aerosol Load in the Stratosphere Linked to Asian Monsoon Transport, Science, 337, 78–81, doi:10.1126/science.1219371, 2012.

Brenot, H., Theys, N., Clarisse, L., van Geffen, J., van Gent, J., Van Roozendael, M., van der A, R., Hurtmans, D., Coheur, P.-F., Clerbaux, C., Valks, P., Hedelt, P., Prata, F., Rasson, O., Sievers, K., and Zehner, C.: Support to Aviation Control Service (SACS): an online service for near-real-time satellite monitoring of volcanic plumes, Nat. Hazards Earth Syst. Sci., 14, 1099–1123, doi:10.5194/nhess-14-1099-2014, 2014.

Brioude, J., Arnold, D., Stohl, A., Cassiani, M., Morton, D., Seibert, P., Angevine, W., Evan, S., Dingwell, A., Fast, J. D., Easter, R. C., Pisso, I., Burkhart, J., and Wotawa, G.: The Lagrangian particle dispersion model FLEXPART-WRF version 3.1, Geosci. Model Dev., 6, 1889–1904, doi:10.5194/gmd-6-1889-2013, 2013.

Clarisse, L., Coheur, P.-F., Theys, N., Hurtmans, D., and Clerbaux, C.: The 2011 Nabro eruption, a SO_2 plume height analysis using IASI measurements, Atmos. Chem. Phys., 14, 3095–3111, doi:10.5194/acp-14-3095-2014, 2014.

De Backer, H. and De Muer, D.: Intercomparison of Total Ozone Data Measured with Dobson and Brewer Ozone Spectrophotometers at Uccle (Belgium) From January 1984 to March 1991, Including Zenith Sky Observations, J. Geophys. Res., 96, 20711–20719, 1991.

Durant, A. J., Bonadonna, C., and Horwell, C. J.: Atmospheric and environmental impacts of volcanic particulates, Elements, 6, 235–240, 2010.

Engelmann, R., Kanitz, T., Baars, H., Heese, B., Althausen, D., Skupin, A., Wandinger, U., Komppula, M., Stachlewska, I. S., Amiridis, V., Marinou, E., Mattis, I., Linné, H., and Ansmann, A.: The automated multiwavelength Raman polarization and water-vapor lidar Polly^{XT}: the neXT generation, Atmos. Meas. Tech., 9, 1767–1784, doi:10.5194/amt-9-1767-2016, 2016.

Fairlie, T. D., Vernier, J.-P., Natarajan, M., and Bedka, K. M.: Dispersion of the Nabro volcanic plume and its relation to the Asian summer monsoon, Atmos. Chem. Phys., 14, 7045–7057, doi:10.5194/acp-14-7045-2014, 2014.

Fioletov, V. E., Griffioen, E., Kerr, J. B., and Wardle, D. I.: Influence of volcanic sulfur dioxide on spectral UV irradiance as measured by Brewer Spectrophotometers, Geophys. Res. Lett., 25, 1665–1668, 1998.

Fioletov, V. E., McLinden, C. A., Krotkov, N., Moran, M. D., and Yang, K.: Estimation of SO_2 emissions using OMI retrievals, Geophys. Res. Lett., 38, L21811, doi:10.1029/2011GL049402, 2011.

Fioletov, V. E., McLinden, C. A., Krotkov, N., Yang, K., Loyola, D. G., Valks, P., Theys, N., Van Roozendael, M., Nowlan, C. R., Chance, K., Liu, X., Lee, C., and Martin, R. V.: Application of OMI, SCIAMACHY, and GOME-2 satellite SO_2 retrievals for detection of large emission sources, J. Geophys. Res., 118, 1–20, doi:10.1002/jgrd.50826, 2013.

Fioletov, V. E., McLinden, C. A., Cede, A., Davies, J., Mihele, C., Netcheva, S., Li, S.-M., and O'Brien, J.: Sulfur dioxide (SO_2) vertical column density measurements by Pandora spectrometer over the Canadian oil sands, Atmos. Meas. Tech., 9, 2961–2976, doi:10.5194/amt-9-2961-2016, 2016.

Flemming, J. and Inness, A.: Volcanic sulfur dioxide plume forecasts based on UV satellite retrievals for the 2011 Grímsvötn and the 2010 Eyjafjallajökull eruption, J. Geophys. Res.-Atmos., 118, 10172–10189, doi:10.1002/jgrd.50753, 2013.

Flemming, J., Huijnen, V., Arteta, J., Bechtold, P., Beljaars, A., Blechschmidt, A.-M., Diamantakis, M., Engelen, R. J., Gaudel, A., Inness, A., Jones, L., Josse, B., Katragkou, E., Marecal, V., Peuch, V.-H., Richter, A., Schultz, M. G., Stein, O., and Tsikerdekis, A.: Tropospheric chemistry in the Integrated Forecasting System of ECMWF, Geosci. Model Dev., 8, 975–1003, doi:10.5194/gmd-8-975-2015, 2015.

Flentje, H., Claude, H., Elste, T., Gilge, S., Köhler, U., Plass-Dülmer, C., Steinbrecht, W., Thomas, W., Werner, A., and Fricke, W.: The Eyjafjallajökull eruption in April 2010 – detection of volcanic plume using in-situ measurements, ozone sondes and lidar-ceilometer profiles, Atmos. Chem. Phys., 10, 10085-10092, doi:10.5194/acp-10-10085-2010, 2010.

Gíslason, S. R., Stefánsdóttir, G., Pfeffer, M. A., Barsotti, S., Jóhannsson, Th., Galeczka, I., Bali, E., Sigmarsson, O., Stefánsson, A., Keller, N. S., Sigurdsson, Á., Bergsson, B., Galle, B., Jacobo, V. C., Arellano, S., Aiuppa, A., Jónasdóttir, E. B., Eiríksdóttir, E. S., Jakobsson, S., Guðfinnsson, G. H., Halldórsson, S. A., Gunnarsson, H., Haddadi, B., Jónsdóttir, I., Thordarson, Th., Riishuus, M., Högnadóttir, Th., Dürig, T., Pedersen, G. B. M., Höskuldsson, Á., and Gudmundsson, M. T.: Environmental pressure from the 2014–15 eruption of Bárðarbunga volcano, Iceland, Geochem. Persp. Let., 1, 84–93, 2015.

Haywood, J. M., Jones, A., Clarisse, L., Bourassa, A., Barnes, J., Telford, P., Bellouin, N., Boucher, O., Agnew, P., Clerbaux, C., Coheur, P., Degenstein, D., and Braesickeieven, P.: Observations

of the eruption of the Sarychev volcano and simulations using the HadGEM2 climate model, J. Geophys. Res., 115, D21212, doi:10.1029/2010JD014447, 2010.

Ialongo, I., Hakkarainen, J., Kivi, R., Anttila, P., Krotkov, N. A., Yang, K., Li, C., Tukiainen, S., Hassinen, S., and Tamminen, J.: Comparison of operational satellite SO_2 products with ground-based observations in northern Finland during the Icelandic Holuhraun fissure eruption, Atmos. Meas. Tech., 8, 2279–2289, doi:10.5194/amt-8-2279-2015, 2015.

Inness, A., Blechschmidt, A.-M., Bouarar, I., Chabrillat, S., Crepulja, M., Engelen, R. J., Eskes, H., Flemming, J., Gaudel, A., Hendrick, F., Huijnen, V., Jones, L., Kapsomenakis, J., Katragkou, E., Keppens, A., Langerock, B., de Mazière, M., Melas, D., Parrington, M., Peuch, V. H., Razinger, M., Richter, A., Schultz, M. G., Suttie, M., Thouret, V., Vrekoussis, M., Wagner, A., and Zerefos, C.: Data assimilation of satellite-retrieved ozone, carbon monoxide and nitrogen dioxide with ECMWF's Composition-IFS, Atmos. Chem. Phys., 15, 5275–5303, doi:10.5194/acp-15-5275-2015, 2015.

Joly, M. and Peuch, V.-H.: Objective classification of air quality monitoring sites over Europe, Atmos. Environ., 47, 111–123, 2012.

Kerr, J. B.: New methodology for deriving total ozone and other atmospheric variables from Brewer spectrophotometer direct sun spectra, J. Geophys. Res., 107, 4731, doi:10.1029/2001JD001227, 2002.

Kerr, J. B.: The Brewer Spectrophotometer, in: UV Radiation in Global Climate Change: Measurements, Modeling and Effects on Ecosystems, edited by: Gao, W., Schmoldt, D. L., and Slusser, J. R., Tsinghua University Press, Beijing and Springer-Verlag Berlin Heidelberg, 160–191, ISBN 978-7-302-20360-5, 2010.

Kerr, J. B., McElroy, C. T., and Olafson, R. A.: Measurements of ozone with the Brewer ozone spectrophotometer, Proceedings of the Quadrennial Ozone Symposium, Boulder, Colorado, edited by: London, J., National Center for Atmospheric Research, Boulder, Colorado, 74–79, 1980.

Kerr, J. B., Evans, W. F. J., and Ashbridge, I. A.: Recalibration of Dobson field spectrophotometers with a travelling Brewer spectrophotometer standard, in: Atmospheric Ozone, Proceedings of the Quadrennial Ozone Symposium, Halkidiki, Greece, 3–7 September 1984, edited by: Zerefos, C. S. and Ghazi, A., D. Reidel Publishing Company, Hingham, Mass., 381–386, 1985.

Kerr, J. B., Asbridge, I. A., and Evans, W. F. J.: Intercomparison of Total Ozone Measured by the Brewer and Dobson Spectrophotometers at Toronto, J. Geophys. Res., 93, 11129–11140, 1988.

Kokkalis, P., Papayannis, A., Amiridis, V., Mamouri, R. E., Veselovskii, I., Kolgotin, A., Tsaknakis, G., Kristiansen, N. I., Stohl, A., and Mona, L.: Optical, microphysical, mass and geometrical properties of aged volcanic particles observed over Athens, Greece, during the Eyjafjallajökull eruption in April 2010 through synergy of Raman lidar and sunphotometer measurements, Atmos. Chem. Phys., 13, 9303–9320, doi:10.5194/acp-13-9303-2013, 2013.

Koukouli, M. E., Clarisse, L., Carboni, E., Van Gent J., Spinetti, C., Balis, D., Dimopoulos S., Grainger, R., Theys, N., Tampellini, L., and Zehner, C.: Intercomparison of Metop-A SO_2 measurements during the 2010–2011 Icelandic eruptions, Ann. Geophys., 57, 1–6, doi:10.4401/ag-6613, 2014.

Kristiansen, N. I., Stohl, A., Prata, A. J., Richter, A., Eckhardt, S., Seibert, P., Hoffmann, A., Ritter, C., Bitar, L., Duck, T. J., and Stebel, K.: Remote sensing and inverse transport modeling of the Kasatochi eruption sulfur dioxide cloud, J. Geophys. Res., 115, D00L16, doi:10.1029/2009JD013286, 2010.

Kristiansen, N. I., Stohl, A., Prata, A. J., Bukowiecki, N., Dacre, H., Eckhardt, S., Henne, S., Hort, M. C., Johnson, B. T., Marenco, F., Neininger, B., Reitebuch, O., Seibert, P., Thomson D. J., Webster, H. N., and Weinzierl, B.: Performance assessment of a volcanic ash transport model mini-ensemble used for inverse modeling of the 2010 Eyjafjallajökull eruption, J. Geophys. Res., 117, D00U11, doi:10.1029/2011JD016844, 2012.

Krotkov, N. A., Schoeberl, M. R., Morris, G. A., Carn, S., and Yang, K.: Dispersion and lifetime of the SO_2 cloud from the August 2008 Kasatochi eruption, J. Geophys. Res., 115, D00L20, doi:10.1029/2010JD013984, 2010.

Krotkov, N., Yang, K., and Carn, S.: A-Train observations of Nabro (Eritrea) eruption on June 13–16 2011, available at: http://aura.gsfc.nasa.gov/science/feature-20120305b.html (last access: 23 March 2016), 2011.

Kumharn, W., Rimmer, J. S., Smedley, A. R., Ying, T. Y., and Webb, A. R.: Aerosol Optical Depth and the Global Brewer Network: A Study Using UK-and Malaysia-Based Brewer Spectrophotometers, J. Atmos. Ocean. Tech., 29, 857–866, doi:10.1175/JTECH-D-11-00029.1, 2012.

Levelt, P. F., van den Oord, G. H. J., Dobber, M. R., Mälkki, A., Visser, H., de Vries, J., Stammes, P., Lundell, J., and Saari, H.: The ozone monitoring instrument, IEEE T. Geosci. Remote, 44, 1093–1101, doi:10.1109/TGRS.2006.872333, 2006.

Li, C., Joiner, J., Krotkov, N. A., and Bhartia, P. K.: A fast and sensitive new satellite SO_2 retrieval algorithm based on principal component analysis: Application to the ozone monitoring instrument, Geophys. Res. Lett., 40, 6314–6318, doi:10.1002/2013GL058134, 2013.

McLinden, C. A., Fioletov, V., Boersma, K. F., Krotkov, N., Sioris, C. E., Veefkind, J. P., and Yang, K.: Air quality over the Canadian oil sands: a first assessment using satellite observations, Geophys. Res. Lett., 39, L04804, doi:10.1029/2011GL050273, 2012.

Moxnes, E. D., Kristiansen, N. I., Stohl, A., Clarisse, L., Durant, A., Weber, K., and Vogel, A.: Separation of ash and sulfur dioxide during the 2011 Grímsvötn eruption, J. Geophys. Res.-Atmos., 119, 7477–7501, doi:10.1002/2013JD021129, 2014.

Newhall, C. G. and Self, S.: The Volcanic Explosivity Index (VEI): An Estimate of Explosive Magnitude for Historical Volcanism, J. Geophys. Res., 87, 1231–1238, doi:10.1029/JC087iC02p01231, 1982.

Pappalardo, G., Mona, L., D'Amico, G., Wandinger, U., Adam, M., Amodeo, A., Ansmann, A., Apituley, A., Alados Arboledas, L., Balis, D., Boselli, A., Bravo-Aranda, J. A., Chaikovsky, A., Comeron, A., Cuesta, J., De Tomasi, F., Freudenthaler, V., Gausa, M., Giannakaki, E., Giehl, H., Giunta, A., Grigorov, I., Groß, S., Haeffelin, M., Hiebsch, A., Iarlori, M., Lange, D., Linné, H., Madonna, F., Mattis, I., Mamouri, R.-E., McAuliffe, M. A. P., Mitev, V., Molero, F., Navas-Guzman, F., Nicolae, D., Papayannis, A., Perrone, M. R., Pietras, C., Pietruczuk, A., Pisani, G., Preißler, J., Pujadas, M., Rizi, V., Ruth, A. A., Schmidt, J., Schnell, F., Seifert, P., Serikov, I., Sicard, M., Simeonov, V., Spinelli, N., Stebel, K., Tesche, M., Trickl, T., Wang, X., Wagner, F., Wiegner, M., and Wilson, K. M.: Four-dimensional dis-

tribution of the 2010 Eyjafjallajökull volcanic cloud over Europe observed by EARLINET, Atmos. Chem. Phys., 13, 4429–4450, doi:10.5194/acp-13-4429-2013, 2013.

Prata, A. J., Gangale, G., Clarisse, L., and Karagulian, F.: Ash and sulfur dioxide in the 2008 eruptions of Okmok and Kasatochi: Insights from high spectral resolution satellite measurements, J. Geophys. Res., 115, D00L18, doi:10.1029/2009JD013556, 2010.

Rix, M., Valks, P., Hao, N., van Geffen, J., Clerbaux, C., Clarisse, L., Coheur, P.-F., Loyola, D., Erbertseder, T., Zimmer, W., and Emmadi, S.: Satellite monitoring of volcanic sulfur dioxide emissions for early warning of volcanic hazards, IEEE J. Sel. Top. Appl., 2, 196–206, doi:10.1109/JSTARS.2009.2031120, 2009.

Rix, M., Valks, P., Hao, N., Loyola, D., Schlager, H., Huntrieser, H., Flemming, J., Koehler, U., Schumann, U., and Inness, A.: Volcanic SO_2, BrO and plume height estimations using GOME-2 satellite measurements during the eruption of Eyjafjallajökull in May 2010, J. Geophys. Res., 117, D00U19, doi:10.1029/2011JD016718, 2012.

Robock, A.: Volcanic eruptions and climate, Rev. Geophys., 38, 191–219, 2000.

Sawamura, P., Vernier, J. P., Barnes, J. E., Berkoff, T. A., Welton, E. J., Alados-Arboledas, L., Navas-Guzmán, F., Pappalardo, G., Mona, L., Madonna, F., Lange, D., Sicard, M., Godin-Beekmann, S., Payen, G., Wang, Z., Hu, S., Tripathi, S. N., Cordoba-Jabonero, C., and Hoff, R. M.: Stratospheric AOD after the 2011 eruption of Nabro volcano measured by lidars over the Northern Hemisphere, Environ. Res. Lett. 7, 034013, doi:10.1088/1748-9326/7/3/034013, 2012.

Schaefer, S. J., Kerr, J. B., Millán, M. M., Realmuto, V. J., Krueger, A. J., Krotkov, N. A., Seftor, C., and Sprod, I. E.: Geophysicists unite to validate volcanic SO_2 measurements, EOS T. Am. Geophy.s Un., 78, 217–223, 1997.

Schmidt, A., Leadbetter, S., Theys, N., Carboni, E., Witham, C. S., Stevenson, J. A., Birch, C. E., Thordarson, T., Turnock, S., Barsotti, S., Delaney, L., Feng, W., Grainger, R. G., Hort, M. C., Höskuldsson, Á., Ialongo, I., Ilyinskaya, E., Jójannsson, T., Kenny, P., Mather, T. A., Richards, N. A. D., and Shepherd, J.: Satellite detection, long-range transport, and air quality impacts of volcanic sulfur dioxide from the 2014–2015 flood lava eruption at Bárðarbunga (Iceland), J. Geophys. Res.-Atmos., 120, 9739–9757, doi:10.1002/2015JD023638, 2015.

Skamarock, W. C., Klemp, J. B., Dudhia, J., Gill, D. O., Barker, D. M., Duda, M. G., Huang, X.-Y., Wang, W., and Powers, J. G.: A Description of the Advanced Research WRF Version 3, NCAR Technical Note 475, NCAR/TN–475+STR, National Center for Atmospheric Research, Boulder, Colorado, USA, 125 pp., available at: http://www2.mmm.ucar.edu/wrf/users/docs/arw_v3.pdf, 2008.

Spinei, E., Carn, S. A., Krotkov, N. A., Mount, G. H., Yang, K., and Krueger, A. J.: Validation of ozone monitoring instrument SO_2 measurements in the Okmok volcanic cloud over Pullman, WA in July 2008, J. Geophys. Res., 115, D00L08, doi:10.1029/2009JD013492, 2010.

Stein, A. F., Draxler, R. R, Rolph, G. D., Stunder, B. J. B., Cohen, M. D., and Ngan, F.: NOAA's HYSPLIT atmospheric transport and dispersion modeling system, B. Am. Meteor. Soc., 96, 2059–2077, doi:10.1175/BAMS-D-14-00110.1, 2015.

Stohl, A., Forster, C., Frank, A., Seibert, P., and Wotawa, G.: Technical note: The Lagrangian particle dispersion model FLEXPART version 6.2, Atmos. Chem. Phys., 5, 2461–2474, doi:10.5194/acp-5-2461-2005, 2005

Stohl, A., Prata, A. J., Eckhardt, S., Clarisse, L., Durant, A., Henne, S., Kristiansen, N. I., Minikin, A., Schumann, U., Seibert, P., Stebel, K., Thomas, H. E., Thorsteinsson, T., Tørseth, K., and Weinzierl, B.: Determination of time- and height-resolved volcanic ash emissions and their use for quantitative ash dispersion modeling: the 2010 Eyjafjallajökull eruption, Atmos. Chem. Phys., 11, 4333–4351, doi:10.5194/acp-11-4333-2011, 2011.

Telling, J., Flower, V. J. B., and Carn, S. A.: A multi-sensor satellite assessment of SO_2 emissions from the 2012-13 eruption of Plosky Tolbachik volcano, Kamchatka, J. Volcanol. Geoth. Res., 307, 98–106, doi:10.1016/j.jvolgeores.2015.07.010, 2015.

Thomas, H. E. and Prata, A. J.: Sulphur dioxide as a volcanic ash proxy during the April–May 2010 eruption of Eyjafjallajökull Volcano, Iceland, Atmos. Chem. Phys., 11, 6871–6880, doi:10.5194/acp-11-6871-2011, 2011.

Thorsteinsson, T., Jóhannsson, T., Stohl, A., and Kristiansen, N. I.: High levels of particulate matter in Iceland due to direct ash emissions by the Eyjafjallajökull eruption and resuspension of deposited ash, J. Geophys. Res., 117, B00C05, doi:10.1029/2011JB008756, 2012.

Vestreng, V., Myhre, G., Fagerli, H., Reis, S., and Tarrasón, L.: Twenty-five years of continuous sulphur dioxide emission reduction in Europe, Atmos. Chem. Phys., 7, 3663–3681, doi:10.5194/acp-7-3663-2007, 2007.

Waythomas, C. F., Scott, W. E., Prejean, S. G., Schneider, D. J., Izbekov, P., and Nye, C. J.: The 7–8 August 2008 eruption of Kasatochi Volcano central Aleutian Islands, Alaska, J. Geophys. Res., 115, B00B06, doi:10.1029/2010JB007437, 2010.

Webley, P. W., Steensen, T., Stuefer, M., Grell, G., Freitas, S., and Pavolonis, M.: Analyzing the Eyjafjallajökull 2010 eruption using satellite remote sensing, lidar and WRF-Chem dispersion and tracking model, J. Geophys. Res., 117, D00U26, doi:10.1029/2011JD016817, 2012.

Wild, M.: Enlightening global dimming and brightening, B. Am. Meteorol. Soc., 93, 27–37, doi:10.1175/BAMS-D-11-00074.1, 2012.

WMO (World Meteorological Organization): Scientific Assessment of Ozone Depletion: 2010, Global Ozone Research and Monitoring Project, Geneva, Switzerland, Report No. 52, 516 pp., 2011.

WMO (World Meteorological Organization): Scientific Assessment of Ozone Depletion: 2014, Global Ozone Research and Monitoring Project, Geneva, Switzerland, Report No. 55, 416 pp., 2014.

Yang, K., Krotkov, N. A., Krueger, A. J., Carn, S. A., Bhartia, P. K., and Levelt, P. F.: Retrieval of large volcanic SO_2 columns from the aura ozone monitoring instrument: comparison and limitations, J. Geophys. Res., 112, D24S43, doi:10.1029/2007JD008825, 2007.

Zerefos, C., Ganev, K., Kourtidis, K., Tzortziou, M., Vasaras, A., and Syrakov, E.: On the origin of SO_2 above Northern Greece, Geophys. Res. Lett., 27, 365–368, 2000.

Zerefos, C. S., Eleftheratos, K., Meleti, C., Kazadzis, S., Romanou, A., Ichoku, C., Tselioudis, G., and Bais, A.: Solar dimming and brightening over Thessaloniki, Greece, and Beijing, China, Tellus B, 61, 657–665, doi:10.1111/j.1600-0889.2009.00425.x, 2009.

Zerefos, C. S., Tetsis, P., Kazantzidis, A., Amiridis, V., Zerefos, S. C., Luterbacher, J., Eleftheratos, K., Gerasopoulos, E., Kazadzis, S., and Papayannis, A.: Further evidence of important environmental information content in red-to-green ratios as depicted in paintings by great masters, Atmos. Chem. Phys., 14, 2987–3015, doi:10.5194/acp-14-2987-2014, 2014.